

REVISITING COSMOLOGICAL DIFFUSION MODELS IN UNIMODULAR GRAVITY AND THE H_0 TENSION

A PREPRINT

Francisco X. Linares Cedeño^{a b †} and Ulises Nucamendi^{a b ††}

^aInstituto de Física y Matemáticas, Universidad Michoacana de San Nicolás de Hidalgo, Edificio C-3, Ciudad Universitaria, CP. 58040 Morelia, Michoacán, México.

^bMesoamerican Centre for Theoretical Physics, Universidad Autónoma de Chiapas, Carretera Zapata Km 4, Real del Bosque (Terán), 29040, Tuxla Gutierrez, Chiapas, México.

[†]francisco.linares@umich.mx , ^{††}unucamendi@gmail.com

April 8, 2024

ABSTRACT

Within the framework of Unimodular Gravity, we consider non-gravitational interactions between dark matter and dark energy. Particularly, we describe such interactions in the dark sector by considering diffusion models that couple the cold dark matter fluid with the dark energy component, where the latter has the form of a variable cosmological “constant”. For the first time, we solve the cosmological evolution for these models from the radiation domination era to the present day. We show how the diffusion processes take place by analyzing the cosmological evolution of the energy density parameters Ω_{cdm} and Ω_Λ , as well as that of the Hubble parameter. Finally, we perform the statistical analysis, imposing constraints on the diffusion parameters, by using data from Planck 2018, SH0ES, Pantheon, and HOLICOW collaborations. We found that cosmological diffusion models in the framework of Unimodular Gravity can ease the current tension in the value of H_0 .

Keywords Unimodular Gravity · Interacting dark sector · H_0 tension

1 Introduction

After more than 100 years, General Relativity (GR) remains as the theory successfully describing the gravitational interactions [1, 2]. In the cosmological context, GR offers a mathematical ground that has allowed to describe the evolution of the Universe, from the era when the first atomic nuclei form, to the current phase of accelerated expansion. Such description lies within the standard cosmological model Λ CDM, which demands, however, a new particle for the so-called *Cold Dark Matter* (CDM) component, responsible for the structure formation process, and which interacts mostly gravitationally with the rest of the known particles. The other ingredient of this model is the *Cosmological Constant* Λ , which is required to explain the current accelerated expansion of the Universe. Thus, GR is a successful gravitational framework to describe the evolution of the Universe as long as a new *dark sector* (dark matter particles as well as a cosmological constant) is added.

With the aim of gaining some theoretical understanding on what these new components of the Universe might be, other approaches have been proposed, such as modifying or including new contributions to the Einstein-Hilbert action. In particular, one of the main motivations to consider alternatives approaches to GR, is the observed current phase of accelerated expansion of the Universe [3, 4, 5, 6, 7], which is thought it is produced by the so-called *Dark Energy* (DE). Many models to explain DE have been proposed, such as fluids with variable equation of state [8, 9, 10, 11, 12, 13, 14, 15], scalar fields [16, 17, 18, 19, 20, 21, 22, 23, 24, 25, 26, 27, 28, 29], modified gravity [30, 31, 32, 33, 34, 35]. However, it seems that the most favored explanation according to several observations, is the cosmological constant term Λ in the Einstein field equations,

$$R_{\mu\nu} - \frac{1}{2}Rg_{\mu\nu} + \Lambda g_{\mu\nu} = \kappa^2 T_{\mu\nu}, \quad (1)$$

where $\kappa^2 = 8\pi G$. Historically, with the aim of having a quasi-static matter distribution in the Universe, Einstein introduced by-hand the term Λ in his field equations [36]. After Edwin Hubble's observations of how distant galaxies are receding away from us [37], and later with the discovery of the accelerating expansion of the Universe through supernovae observations [3, 4], the cosmological constant plays the role of the DE component responsible for such accelerated expansion that the Universe is currently experiencing. Its origin and physical interpretation have been debated and speculated since then, giving rise to the different approaches mentioned above.

One of the proposal for a possible origin of Λ that is being currently studied with great interest, is related with the original formulation of the field equations of GR, where Einstein showed that it is always possible to consider a choice of coordinate such that the determinant of the metric tensor is fixed [38]. Specifically, when the determinant g of the metric tensor $g_{\mu\nu}$ satisfies the *unimodular condition* $\sqrt{-g} = 1$, the Einstein tensor gets a simplified form. Later, in trying to understand the role of gravitational forces in the constitution of matter, Einstein showed that in a formulation of the field equations freed of the scalar of curvature $R \equiv g^{\mu\nu} R_{\mu\nu}$, the cosmological constant term can arise as an integration constant [39].

A link between the condition of a fixed metric determinant and the cosmological constant, was made for the first time in [40], where the authors consider unimodular coordinate mappings, this is, $x^\mu \rightarrow x'^\mu$ for which $\det |\partial x'^\mu / \partial x^\nu| = 1$. Then, with the aim of building a theory considering such coordinate transformations, they add the unimodular condition to the Einstein-Hilbert action through a Lagrange multiplier λ ,

$$S = S_{EH} + S_\lambda = \frac{1}{\kappa^2} \int d^4x \sqrt{-g} R + \frac{1}{\kappa^2} \int d^4x \lambda(x) (\sqrt{-g} - 1), \quad (2)$$

which after variation with respect to the inverse of the metric tensor $g^{\mu\nu}$ leads to

$$R_{\mu\nu} - \frac{1}{2} R g_{\mu\nu} + \lambda g_{\mu\nu} = 0. \quad (3)$$

Taking the trace of Eq. (3), the Lagrange multiplier is determined to be

$$\lambda = \frac{1}{4} R, \quad (4)$$

and therefore, Eq. (3) is written as

$$R_{\mu\nu} - \frac{1}{4} R g_{\mu\nu} = 0. \quad (5)$$

When considering matter content S_M in the action (2), Eqs. (3) and (4) are given by

$$R_{\mu\nu} - \frac{1}{2} R g_{\mu\nu} + \lambda g_{\mu\nu} = \kappa^2 T_{\mu\nu}, \quad \lambda = \frac{1}{4} (R + \kappa^2 T), \quad (6)$$

where $T_{\mu\nu} = -2g^{-1/2} \delta S_M / \delta g^{\mu\nu}$ is the energy-momentum tensor, and T its trace. After eliminating λ , we have

$$R_{\mu\nu} - \frac{1}{4} R g_{\mu\nu} = \kappa^2 \left(T_{\mu\nu} - \frac{1}{4} T g_{\mu\nu} \right), \quad (7)$$

which is the trace-free version of the Einstein field equations. This theory leading to the new set of equations (7) for the gravitational field has been dubbed *Unimodular Gravity* (UG). First works in UG are [40, 41, 42, 43, 44, 45], approaches of UG in the quantum regime have been explored by [46, 47, 48, 49, 50], and some recent cosmological applications have been studied in [51, 52, 53, 54, 55, 56, 57, 58, 59].

One of the main features of this theory can be seen as follows: notice that we can rewrite Eq. (7) in the following way,

$$G^\mu{}_\nu + \frac{1}{4} (R + \kappa^2 T) \delta^\mu{}_\nu = \kappa^2 T^\mu{}_\nu, \quad (8)$$

where we have introduced the Einstein tensor $G^\mu{}_\nu \equiv R^\mu{}_\nu - \frac{1}{2} R \delta^\mu{}_\nu$. Then, applying the Bianchi identities we have

$$\nabla_\mu G^\mu{}_\nu + \frac{1}{4} \nabla_\nu (R + \kappa^2 T) = \kappa^2 \nabla_\mu T^\mu{}_\nu. \quad (9)$$

Whereas the first term still is identically zero (as in GR), the covariant derivative of the energy-momentum tensor is no longer, in general, locally conserved,

$$\kappa^2 \nabla_\mu T^\mu{}_\nu = \frac{1}{4} \partial_\nu (R + \kappa^2 T) \Rightarrow \lambda(x) \equiv \Lambda + \int_l J, \quad (10)$$

where Λ is an integration constant, and $J_\nu \equiv \kappa^2 \nabla_\mu T^\mu_\nu$ is the energy–momentum current violation to be integrated on some arbitrary path l . Replacing this result into Eq. (6), we have

$$R_{\mu\nu} - \frac{1}{2} R g_{\mu\nu} + \left(\Lambda + \int_l J(x) \right) g_{\mu\nu} = \kappa^2 T_{\mu\nu}. \quad (11)$$

The physical interpretation of the Lagrange multiplier λ is now apparent: it plays the role of an effective cosmological “constant”. In fact, in the particular case when the energy–momentum tensor is conserved ($J = 0$), the integration constant Λ is identified as the cosmological constant term in the Einstein field equations (1). Thus, within the framework of UG, the cosmological constant Λ is not a term introduced by–hand, but it arises naturally as an integration constant when considering the Einstein–Hilbert action with volume-preserving diffeomorphisms¹. However, there will be in general a non–null energy–momentum current violation. Thus, assuming that ordinary matter (photons, neutrinos, baryons) interact only gravitationally with the dark sector, the non-conservation of the energy–momentum tensor leads to a non-gravitational interaction between cold dark matter and the cosmological constant.

Interactions between the components of the dark sector have been studied broadly in the literature [62, 63, 64, 65, 66, 67, 68, 69, 70, 71, 72, 73, 74, 75, 76, 77, 78], and they have shown to be useful as alternative models to Λ CDM, to address the discrepancies found in the measurements of the current value of the Hubble parameter H_0 , when it is inferred from early and late Universe observations [79, 80, 81, 82, 83, 84, 85, 86]. We will refer to such discrepancy as the H_0 tension (for recent discussions see [87, 88]). In Figure 1 it can be seen the current value of the Hubble parameter according different experiments. Whereas from observations of the early Universe, based on the Cosmic Microwave Background (CMB), a value of $H_0^{\text{early}} \simeq 68 \text{ km s}^{-1} \text{ Mpc}^{-1}$ is inferred, the combined late Universe observations indicate that $H_0^{\text{late}} \simeq 73 \text{ km s}^{-1} \text{ Mpc}^{-1}$. This discrepancy may be due to systematic errors in the observations, but it can also be suggesting to look for extensions of the Λ CDM model with the aim of exploring new physics.

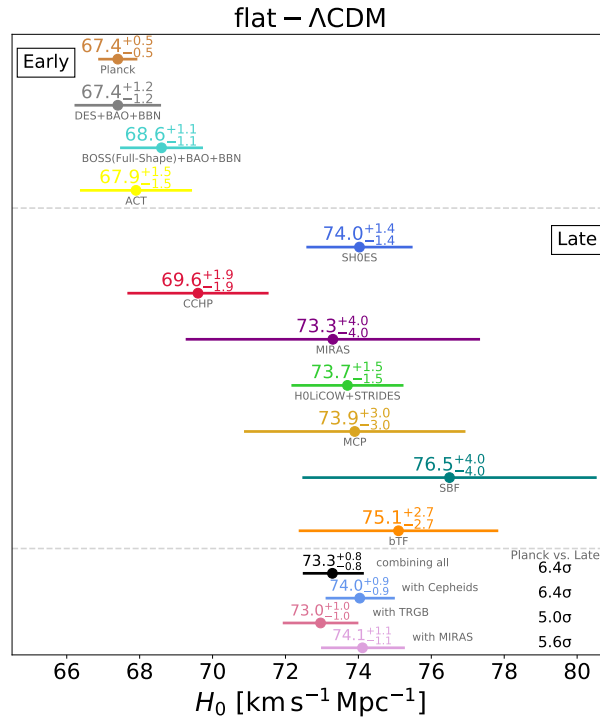


Figure 1: Value of H_0 from different observations. Top: H_0 from CMB observations. Middle: H_0 from late time observations. Bottom: combined late time observations and the corresponding H_0 tension with early time measurements. Data from CMB [7, 89], BAO and BBN [90, 91], SNe Ia and Cepheids [92], SNe Ia and TRGB [93, 94], SNe Ia and Mira variables [95], lensed quasars [96], water megamasers [97], SBF and Cepheids [98]. This is an updated version of Figure 1 from [88]. Credits to Vivien Bonvin and Martin Millon [99].

¹Theoretical analysis on the viability of UG for astrophysical and cosmological applications, as well as discussions about the integrability of J_ν are discussed in [60] and [61] respectively.

Non-gravitational interactions between dark matter and dark energy have been studied through *diffusion models* in the cosmological context within the framework of General Relativity [100, 101], as well as in the context of Two Measure Theories and dynamical spacetime theories [102, 103, 104]. We are particularly interested in diffusion models as those presented in [58, 59], where the authors explore cosmological diffusion processes in the framework of Unimodular Gravity. Specifically we will go further in the analysis by studying these models not only at late times, but from very early times deep within the radiation dominated era. This requires to consider the radiation component into account, which will be important in order to constraint the diffusion models we are interesting in with CMB data.

Thus, in this work we will study diffusion processes between the dark sector components within the framework of Unimodular Gravity. For the first time, these diffusion models are studied in a more realistic cosmological scenario, in which the component of radiation due to the presence of photons and ultra-relativistic neutrinos at early times, is taken into account. Since we will be focused on how these models can alleviate the H_0 tension, it is important to include the radiation component in order to use data from the CMB, and thus being able to test each diffusion model at the last scattering surface ($z_* \simeq 1100$). By performing a statistical analysis we will infer the most likely values of the diffusion models parameters in the light of current astrophysical and cosmological data. This will allow us to analyze the viability of such diffusion models as a possible solution to the H_0 tension. As we will show, the inferred value of H_0 at early times can be in agreement with that obtained from late time observations.

The outline of the present work is the following: in Section 2 we show the cosmological equations for the background evolution within the framework of UG. We analyze the cosmological evolution for each of the diffusion models of interest, studying the diffusion process in terms of the energy density parameters Ω_{cdm} and Ω_Λ . Considering that the current values for each energy density parameter $\Omega_{0,i}$, and for H_0 are those determined by CMB observations (and thus $H_0 = H_0^{early}$ for Λ CDM), we show how the evolution of the Hubble parameter $H(z)$ for each diffusion model gives a current value H_0 consistent with the reported value from local observations, i.e., $H_0 = H_0^{late}$. In particular, when the parameters of the diffusion models are set to zero, we recover the Λ CDM results. We perform the statistical analysis in Section 3, where we: 1) consider only CMB observations from the Planck Compressed 2018 data, and then 2) we include into the analysis observations from the local Universe as those from Cepheids, Supernovae and lensed quasars. In the first analysis, the tension on the H_0 value is eased because the anticorrelation between Ω_{cdm} and H_0 gets a broader range of values due to the presence of the new diffusion parameters. In the second analysis, we obtain that the local observations allow the diffusion models to ease the H_0 tension by shifting the mean value from H_0^{early} to H_0^{late} , and thus, the diffusion models make CMB and late times observations to be in agreement in the value of the Hubble parameter at $z = 0$. Finally, in Section 4 we discuss our results and give some conclusions of our analysis.

2 Background cosmological equations with diffusion

We start by considering a spatially-flat Friedmann-Robertson-Walker (FRW) line element,

$$ds^2 = -dt^2 + a^2(t) [dr^2 + r^2 (d\theta^2 + \sin^2 \theta d\phi^2)] , \quad (12)$$

where the scale factor $a(t)$ is function of the cosmic time t . When considering the FRW line element (12), we are assuming that at large scales the Cosmological Principle is valid, and then both homogeneity and isotropy imply that the effective cosmological constant (10) is now a function of the cosmic time only,

$$\Lambda(t) \equiv \Lambda + \int_t J(t) , \quad (13)$$

where we have replaced the notation $\lambda(t) \rightarrow \Lambda(t)$. The Einstein field equations (11) for the background evolution are given by,

$$H^2 = \frac{\kappa^2}{3} (\rho_\gamma + \rho_\nu + \rho_b + \rho_{cdm} + \rho_{\Lambda(t)}) , \quad (14a)$$

$$\dot{H} = -\frac{\kappa^2}{2} [(\rho_\gamma + p_\gamma) + (\rho_\nu + p_\nu) + (\rho_b + p_b) + (\rho_{cdm} + p_{cdm})] , \quad (14b)$$

$$\dot{\rho}_\gamma = -3H(\rho_\gamma + p_\gamma) , \quad \dot{\rho}_\nu = -3H(\rho_\nu + p_\nu) , \quad \dot{\rho}_b = -3H(\rho_b + p_b) , \quad (14c)$$

$$\dot{\rho}_{cdm} = -3H(\rho_{cdm} + p_{cdm}) - \frac{\dot{\Lambda}(t)}{\kappa^2} . \quad (14d)$$

The dot denotes derivative with respect to cosmic time t , and $H = \dot{a}/a$ is the Hubble parameter. We will consider that baryons (b) and cold dark matter (cdm) behave as dust, and then they have vanishing pressure $p_b = p_{cdm} = 0$, whereas for photons (γ) and ultra-relativistic neutrinos (ν) we have $p_\gamma = \rho_\gamma/3$ and $p_\nu = \rho_\nu/3$.

2.1 Diffusion models

Given a particular form of the cold dark matter energy density $\rho_{cdm}(t)$, Eq. (14d) can be integrated to find the function $\Lambda(t)$. With this approach, here we analyze two diffusion models previously studied in [58]: *Sudden Transfer Model* (STM) and *Anomalous Decay of the Matter Density* (ADMD). Both models are described in terms of two parameters, one regulating the amplitudes of ρ_{cdm} and ρ_Λ (α for STM and γ for ADMD), and other one for the characteristic redshift z^* at which the diffusion process takes place.

Another way to solve (14d) is by explicitly proposing a particular form for the *diffusion function* Q , which is defined as follows,

$$Q(x) \equiv \frac{1}{\kappa^2} \int_l J(x), \quad (15)$$

and thus, the integrated energy–momentum current violation is expressed in terms of the diffusion function $Q(x)$. Given homogeneity and isotropy, this function will depend only on the cosmic time t . Therefore, what we have denoted by $\Lambda(t)$ in Eq. (13) can now be written as

$$\Lambda(t) \equiv \Lambda + \kappa^2 Q(t), \quad (16)$$

in whose case, Eq. (14d) reads

$$\dot{\rho}_{cdm} = -3H(\rho_{cdm} + p_{cdm}) - \dot{Q}(t). \quad (17)$$

An explicit functional form for the diffusion function Q can be given, in order to find the CDM energy density by solving Eq. (17). This was considered by the authors in [59], where two phenomenological models are studied: *Barotropic Model* (BM) and *Continuous Spontaneous Localization* (CSL). Different from the previous two models, only one parameter characterizes the BM and CSL models (x_{cdm} for BM and ξ_{CSL} for CSL).

In this Section we will analyze the cosmological evolution of these four models mentioned above, from the radiation dominated era until the present day. To do so, we will solve the background equations (14) with the Boltzmann code CLASS [105].

2.1.1 Model 1: Sudden Transfer Model

The energy density proposed for the CDM component is given by

$$\rho_{cdm}(z) = \rho_{0,cdm}(1+z)^3 \times \begin{cases} 1 & \text{if } z \geq z^*, \\ 1 - \alpha & \text{if } z < z^*, \end{cases} \quad (18a)$$

where α is the dimensionless diffusion constant controlling the amplitude of the energy transfer, and z^* is the characteristic redshift at which the sudden diffusion process takes place. After integration of Eq. (14d) (with $p_{cdm} = 0$), the effective cosmological constant is given by

$$\Lambda(z) = \begin{cases} \Lambda & \text{if } z \geq z^*, \\ \Lambda + 3H_0^2 \alpha (1+z^*)^3 \Omega_{0,cdm} & \text{if } z < z^*, \end{cases} \quad (18b)$$

and then, once $z < z^*$, the Friedmann equation (14a) can be written as

$$E(z) \equiv \frac{H(z)}{H_0} = \sqrt{\Omega_{0,r}(1+z)^4 + \Omega_b h^2 (1+z)^3 + \Omega_{cdm}(1+z)^3 \left[1 - \alpha + \alpha \left(\frac{1+z^*}{1+z} \right)^3 \right] + \Omega_\Lambda}. \quad (18c)$$

Thus, the diffusion process allows to have different present values of Ω_Λ and Ω_{cdm} for given values of α and z^* . This implies that the current Hubble parameter H_0 can also change its value since it is defined implicitly in the energy density parameters. It can be seen that the standard Friedmann equation is recovered when $\alpha = 0$.

In order to illustrate the diffusion process between CDM and Λ , we have considered the diffusion parameters given by $\{\alpha, z^*\} = \{0.8, 1\}$. As expected, the energy density for cold dark matter (yellow line) drops suddenly at z^* (vertical dash-dotted black line), and the energy density for Λ (red line) increases, as it is shown in Figure 2. The rest of the matter components evolve as usual. Only for comparison, we also have included the standard evolution of CDM and Λ (black dotted and dashed lines respectively). The Friedman constraint is satisfied during all the cosmological evolution (horizontal gray line), this is, $1 = \sum_i \Omega_i(z)$.

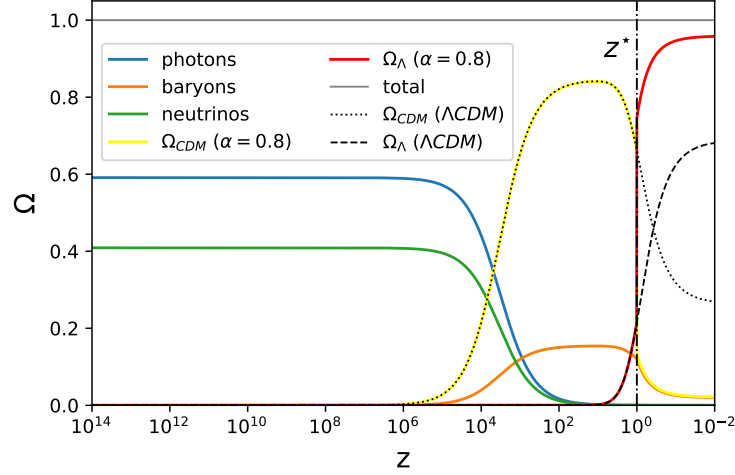


Figure 2: Sudden diffusion between ρ_{cdm} and Λ (Model 1). Whereas photons (blue line), baryons (orange line) and neutrinos (green line) evolve as usual, Ω_{cdm} (yellow line) and Ω_{Λ} (red line) evolve with a diffusion process with $\alpha = 0.8$. The characteristic redshift was settled to $z^* = 1$ (vertical dash-dotted line).

With the aim of exploring the effects of the diffusion process between the dark sector components, different cosmological evolution with several values of the diffusion constant α are shown in Figure 3, where the sudden energy transfer between Ω_{cdm} and Ω_{Λ} can be observed. Particularly, it can be seen that given a characteristic redshift $z^* = 1$ (vertical black line), the diffusion constant α will change the difference between the current values of the energy density parameters for the dark sector. This is expected since α regulates the amount of energy density that the CDM component transfers to the cosmological constant (see Eq. (18a) and (18b)). On the other hand, the effect of different characteristic redshifts z^* on the diffusion process can be seen in Figure 4. We observe that higher values of z^* will lead to lower (larger) values of the cold dark matter (cosmological constant) energy density parameter today.

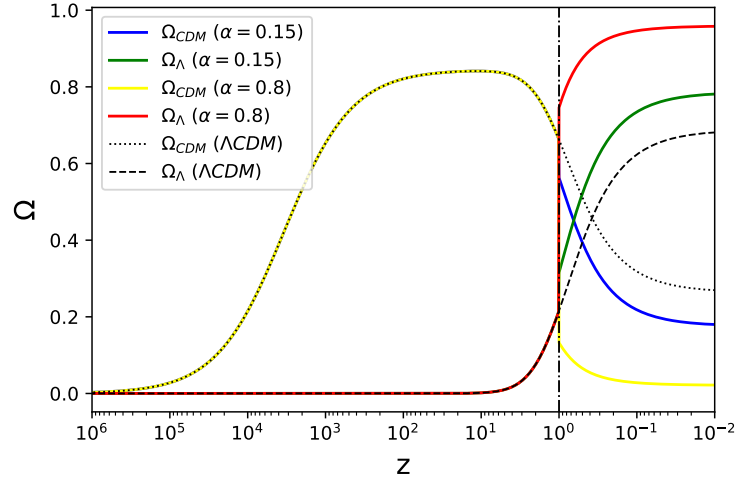


Figure 3: Sudden diffusion between ρ_{cdm} and Λ (Model 1). Black lines show the standard evolution without diffusion ($\alpha = 0$) for CDM (dotted line) and cosmological constant (dashed line). Other lines correspond to a diffusion process with $\alpha = 0.15$ (blue and green lines for CDM and Λ respectively), and $\alpha = 0.8$ (yellow and red lines for CDM and Λ respectively). The characteristic redshift was fixed to $z^* = 1$ (vertical dash-dotted black line).

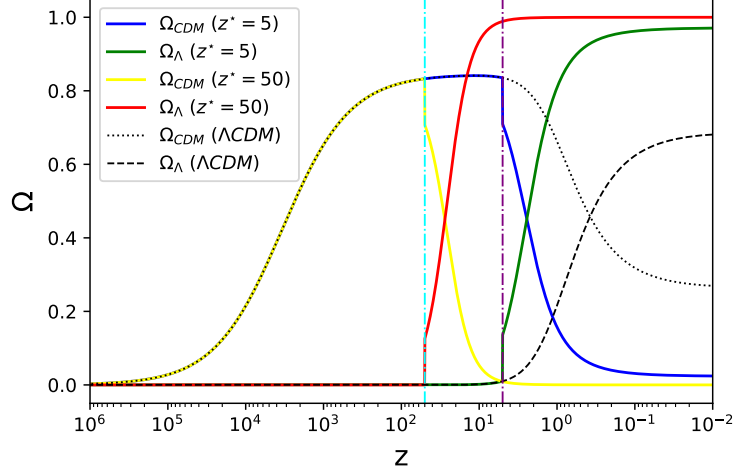


Figure 4: Sudden diffusion between ρ_{cdm} and Λ (Model 1) at different characteristic redshifts: $z^* = 5$ (vertical dash-dotted purple line), and $z^* = 50$ (vertical dash-dotted cyan line). Black lines show the standard evolution without diffusion ($\alpha = 0$) for CDM (dotted line) and cosmological constant (dashed line)). For the diffusion processes between CDM and Λ at $z^* = 5$ (blue and green lines), as well as $z^* = 50$ (yellow and red lines), the diffusion constant was settled to $\alpha = 0.15$.

2.1.2 Model 2: Anomalous Decay of the Matter Density

In this case, the mathematical model for the CDM energy density is proposed to be

$$\rho_{cdm}(z) = \rho_{0,cdm}(1+z)^3 \times \begin{cases} 1 & \text{if } z \geq z^*, \\ \left(\frac{1+z}{1+z^*}\right)^\gamma & \text{if } z < z^*, \end{cases} \quad (19a)$$

where γ is the dimensionless diffusion constant controlling the power of the energy transfer term, and z^* is again the characteristic redshift, this time indicating when the anomalous decay of dark matter occurs. After integration of Eq. (14d), the energy density for Λ is given by

$$\Lambda(z) = \begin{cases} \Lambda & \text{if } z \geq z^*, \\ \Lambda - \frac{3\gamma}{\gamma+3} H_0^2 \left[\left(\frac{1+z}{1+z^*}\right)^\gamma (1+z)^3 - (1+z^*)^3 \right] \Omega_{0,cdm} & \text{if } z < z^*. \end{cases} \quad (19b)$$

Once $z < z^*$, the Friedmann equation (14a) can be written as

$$E(z) \equiv \frac{H(z)}{H_0} = \sqrt{\Omega_{0,r}(1+z)^4 + \Omega_b h^2 (1+z)^3 + \Omega_{cdm}(1+z)^3 \left[\frac{3}{3+\gamma} \left(\frac{1+z}{1+z^*}\right)^\gamma + \frac{\gamma}{3+\gamma} \left(\frac{1+z^*}{1+z}\right)^3 \right] + \Omega_\Lambda}, \quad (19c)$$

where it can be seen that the Λ CDM scenario is recovered when $\gamma = 0$. Figure 5 shows the evolution of all the matter components present in the Universe, considering a diffusion process described by the ADMD model with $\gamma = 0.2$ at a characteristic redshift $z^* = 1$.

In general, depending on the values of $\{\gamma, z^*\}$, the energy transfer between cold dark matter and Λ will be smoother, or steeper than model 1. This can be seen in Figure 6, where we have settled $z^* = 1$ to explore the effect of γ . We observe that, at this redshift, the transition is smooth for different values of γ (the reader can compare this to the case of sudden energy transfer of Model 1 in Figure 3). The cold dark matter fluid diffuses and the cosmological constant captures this energy, which allows to Ω_Λ to reach larger values in the present day in comparison with the Λ CDM.

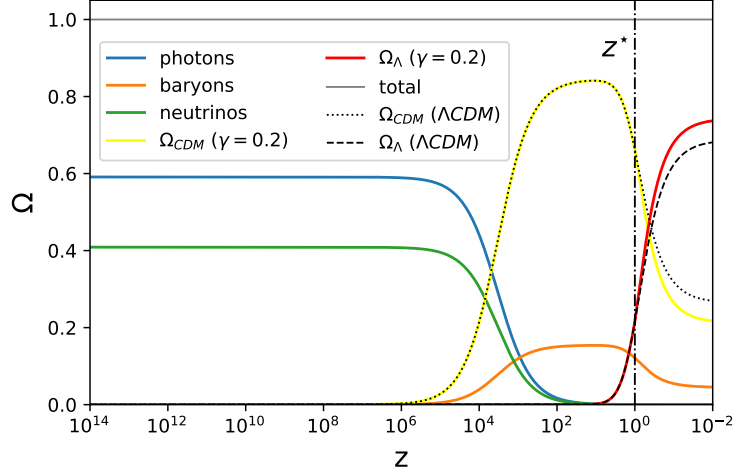


Figure 5: ADMD model for the diffusion between ρ_{cdm} and Λ (Model 2). Photons (blue line), baryons (orange line) and neutrinos (green line) evolve as usual, whereas Ω_{cdm} (yellow line) and Ω_{Λ} (red line) evolve with a diffusion process with $\gamma = 0.2$. The characteristic redshift was set to $z^* = 1$ (vertical dashed line). The horizontal gray line indicates the Friedman constraint $\sum_i \Omega_i(z) = 1$.

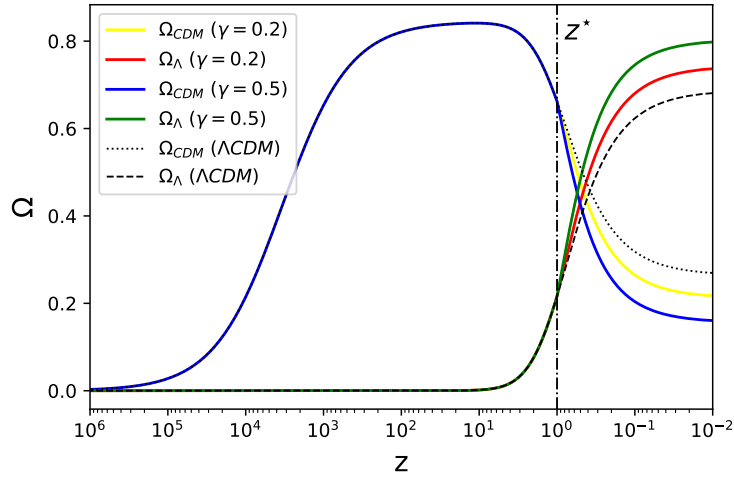


Figure 6: Anomalous decay of cold dark matter density ρ_{cdm} into dark energy Λ (Model 2). Black lines show the standard evolution without diffusion ($\gamma = 0$). Solid lines correspond to a diffusion process with $\gamma = 0.2$ (yellow and red for Ω_{cdm} and Ω_{Λ} respectively), and $\gamma = 0.5$ (blue and green for Ω_{cdm} and Ω_{Λ} respectively). The characteristic redshift was fixed to $z^* = 1$.

The effects of this model on the dark sector energy density parameters due to the characteristic redshift z_* are shown in Figure 7. We can see that the diffusion process induces a steeper fall of the cold dark matter energy density when $z^* = 5, 50$, in comparison to lower characteristic redshifts (for example, at $z^* = 1$ in Figure 6). Besides, the present value of Ω_{cdm} (Ω_Λ) decreases (increases) much more than the cases for lower redshifts.

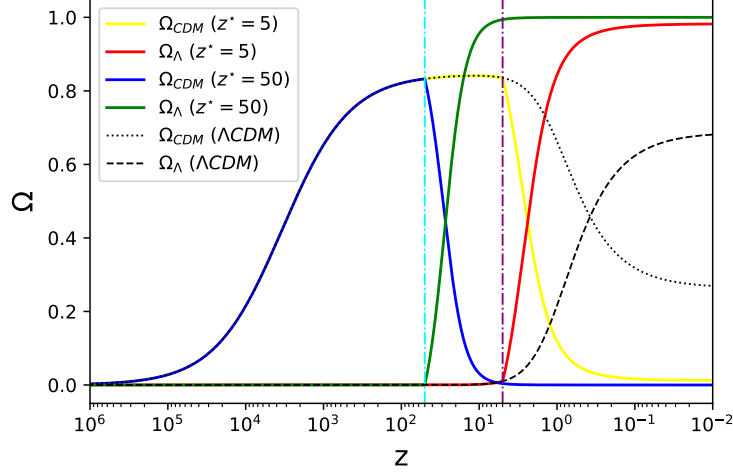


Figure 7: Anomalous decay of cold dark matter density ρ_{cdm} into dark energy Λ (Model 2) at different characteristic redshifts: $z^* = 5$ (vertical dash-dotted purple line), and $z^* = 50$ (vertical dash-dotted cyan line). Black lines show the standard evolution for Ω_{cdm} and Ω_Λ without diffusion ($\gamma = 0$). For the ADMD model, the diffusion constant was settled to $\gamma = 0.5$.

2.1.3 Model 3: Barotropic Model

For the following two models we will solve Eq. (17), for which a diffusion function Q has to be given. One of the forms of this function that has been explored in [59] is

$$Q \equiv x_i \rho_i, \quad (20a)$$

this is, a constant barotropic equation of state x_i relating the energy density of the different matter components ρ_i ($i = b, \gamma, \nu, cdm, \Lambda$) and the diffusion function Q . In our case, the diffusion process will be only due to the CDM component, i.e., $i = cdm$, and thus we have from Eq. (17) that

$$\rho_{cdm}(z) = \rho_{cdm}(1+z)^{\frac{3(\omega_{cdm}+1)}{x_{cdm}+1}}. \quad (20b)$$

The normalized Friedmann equation for this model is given by,

$$E(z) \equiv \frac{H(z)}{H_0} = \sqrt{\Omega_{0,r}(1+z)^4 + \Omega_{0,b}(1+z)^3 + (1+x_{cdm})\Omega_{cdm}(1+z)^{\frac{3}{x_{cdm}+1}} + \Omega_\Lambda}, \quad (20c)$$

where we have considered the standard dust-like behavior for CDM ($\omega_{cdm} \simeq 0$). The cosmological evolution for all matter components is shown in Figure 8, where it can be seen that the diffusion process driven by this model affects to Ω_{cdm} from the moment when its amplitude starts to grow, and during most of the matter domination era. As in the previous models, for comparison we also show the standard Λ CDM case for Ω_{cdm} (black dotted line) and Ω_Λ (black dashed line), but this time we also show the standard evolution of the baryon energy density Ω_b (black dash-dotted line) to show that in the case of the diffusion model (orange line) it increases in the right proportion to balance the CDM contribution (yellow line) such that the total budget of matter still satisfies the Friedmann constraint $\Omega_{tot} = 1$ (gray horizontal line) during all the cosmological evolution.

In Figure 9 we show the evolution of Ω_{cdm} and Ω_Λ for several values of x_{cdm} . Positive values of x_{cdm} (red lines) lead to larger values of Ω_{cdm} at $z = 0$, whereas the current value of the cosmological constant energy density parameter $\Omega_{0,\Lambda}$ decreases (red dashed line). The opposite occurs when negative values of x_{cdm} are considered (green lines).

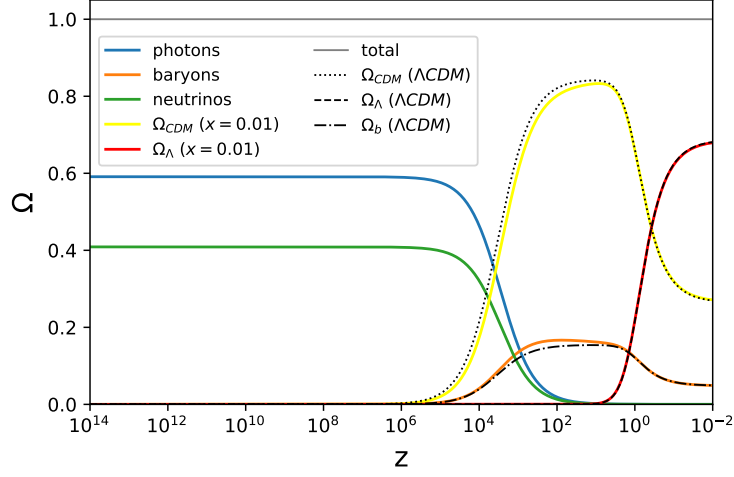


Figure 8: Cosmological evolution of the energy density parameter of each matter component of the Universe considering the diffusion process of Model 3: Barotropic model. The diffusion between CDM and Λ is mediated by the barotropic equation of state $Q = x_{cdm}\rho_{cdm}$.

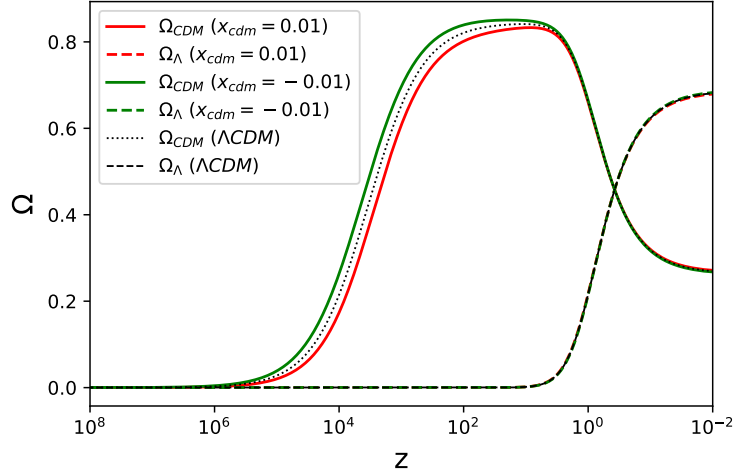


Figure 9: Diffusion between CDM and Λ mediated by the barotropic equation of state $Q = x_{cdm}\rho_{cdm}$. The effect of different values of x_{cdm} can be summarized as an increment (reduction) on Ω_{cdm} for $x_{cdm} > 0$ ($x_{cdm} < 0$). Dotted and dashed black lines represent the standard evolution of Ω_{cdm} and Ω_Λ respectively.

We can see that, different from Models 1 and 2, this model presents diffusion during certain period of time of the cosmological evolution ($z \lesssim 10^6$), and not only at a given characteristic redshift. In this sense, this model could have different implications in the cosmic history, as for example in the matter-radiation equality era z_{eq} , as is shown in Figure 10. In fact, the most notorious effect on the cosmological parameters Ω_{cdm} and Ω_Λ are not at the present day, but approximately from $z \simeq 10^6$ to ~ 5 .

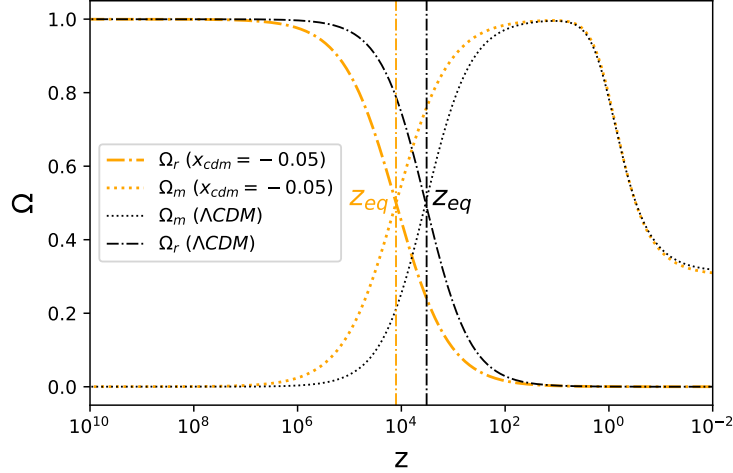


Figure 10: Evolution of Ω_m and Ω_r for the Λ CDM model (black lines) and the barotropic model (orange lines). The redshift for the matter-radiation equality era z_{eq} depends on the diffusion parameter x_{cdm} . For $x_{cdm} = -0.05$, we have $z_{eq} \simeq 12.7 \times 10^3$ (vertical dash-dotted orange line), whereas for Λ CDM we have $z_{eq} \simeq 3.3 \times 10^3$ (vertical dash-dotted black line).

2.1.4 Model 4: Continuous Spontaneous Localization model

An interesting model also studied in [59] is the *Continuous Spontaneous Localization* (CSL) model [106, 107, 108, 109, 110, 111, 112, 113, 61, 114, 115, 116]. This model arises as a proposal to explain the spontaneous collapse of the wave function in quantum mechanics, where the stochastic nature of the collapse is encoded in a new correction term in the Schrödinger equation. Such modification consists in a stochastic noise describing a diffusion process of the wavefunction in Hilbert space. The source of such noise can be of cosmological origin, for instance, due to the dark matter component in the Universe [117, 118]. In the case we are interested in, the predicted form of the diffusion function Q according to the CSL model is [59]

$$\dot{Q} = -\xi_{CSL} \rho_{cdm}, \quad (21a)$$

where ξ_{CSL} is the localization rate, which is interpreted as the frequency of the localization events. After integration of the above expression we have,

$$Q(t) = Q_i - \xi_{CSL} \int_0^t \rho_{cdm}(t') dt', \quad (21b)$$

where $Q_i = Q(t=0)$ is an integration constant that will contribute to the total dark energy density, as we will show. The CDM energy density is then given by,

$$\rho_{cdm}(z) = \rho_{cdm}(1+z)^3 e^{\xi_{CSL} t}, \quad (21c)$$

which lead to the following Friedmann equation,

$$E(z) \equiv \frac{H(z)}{H_0} = \sqrt{\Omega_{0,r}(1+z)^4 + \Omega_b h^2 (1+z)^3 + \Omega_{cdm} \left[e^{\xi_{CSL} t} (1+z)^3 - \xi_{CSL} \int_0^t e^{\xi_{CSL} t'} [1+z(t')]^3 dt' \right] + \Omega_{\Lambda_{eff}}}, \quad (21d)$$

where $\Omega_{\Lambda_{eff}} \equiv \Omega_{\Lambda} + (\kappa^2 Q_i / 3H_0^2)$. Once implemented a generalized form of the *lower incomplete Gamma function* to deal with the integral in the above expression, the Friedmann equation can be written as follows (see Appendix A)

$$E(z) = \begin{cases} \sqrt{\Omega_r(z) + \Omega_b(z) + \Omega_{cdm}(z) [e^{-u_0(1+z)^{-2}} + 2u_0(1+z)^{-2}] + \Omega_{\Lambda_{eff}}}, & \text{for Radiation domination,} \\ \sqrt{\Omega_r(z) + \Omega_b(z) + \Omega_{cdm}(z) [e^{-u_0(1+z)^{-3/2}} - u_0(1+z)^{-3/2}] + \Omega_{\Lambda_{eff}}}, & \text{for Matter domination.} \end{cases} \quad (21e)$$

The evolution of each $\Omega_i(z)$ is shown in Figure 11. Notice that we have introduced a dimensionless parameter $u_0 \equiv -\xi_{CSL} t_0$, where t_0 is the current age of the Universe. It seems that the condition $\xi_{CSL} \leq 0$ is required in order to have physically consistent cosmological evolution for this diffusion model during radiation domination era. We will consider, however, both positive and negative values of u_0 in our analysis. For more details see Appendix A.

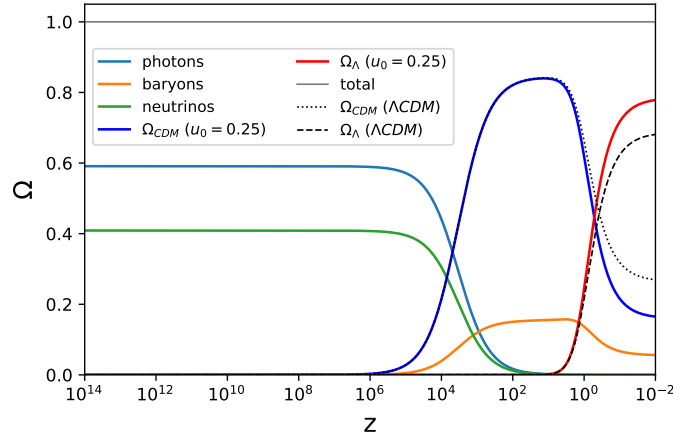


Figure 11: Energy density parameter of each matter component of the Universe as function of the redshift considering the CSL diffusion process. As in previous Figures, the horizontal gray line stands for $\sum_i \Omega_i(z) = 1$.

The sign of the diffusion parameter affects the behavior of both Ω_{cdm} and Ω_{Λ} . This can be seen in Figure 12, where $u_0 > 0$ (blue lines) increases the energy density for the cosmological constant as CDM decreases. The opposite occurs for $u_0 < 0$ (orange lines).

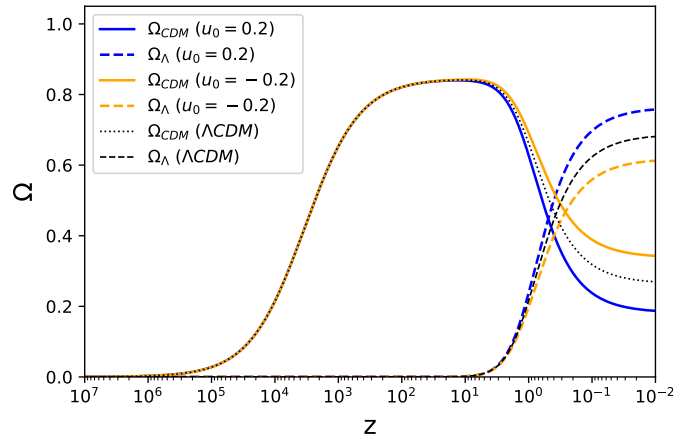


Figure 12: $\Omega_{cdm}(z)$ and $\Omega_{\Lambda}(z)$ for the CSL model for $u_0 = -0.2, 0.2$. Black lines indicate the standard Λ CDM result.

As we mentioned before, all these changes in Ω_{cdm} and Ω_Λ due to the diffusion processes will affect the current value of the Hubble parameter. In particular, if the current values for each energy density parameter $\Omega_{0,i}$ ($i = b, \gamma, \nu, cdm, \Lambda$), as well as for H_0 are those obtained from CMB observations (and thus $H_0 = H_0^{early}$ for Λ CDM), it is possible to find values of the diffusion parameters such that H_0 shifts to the value inferred from late time observations, i.e., $H_0 = H_0^{late}$. We show the evolution of the Hubble parameter in Figure 13. Considering particular values for the parameters of each of the diffusion models studied, we show that it is possible to obtain a cosmological solution for $H(z)$ consistent with the reported value of H_0 from local observations. Once the diffusion parameters are set to zero, the Λ CDM case is recovered and $H_0 = H_0^{early}$.

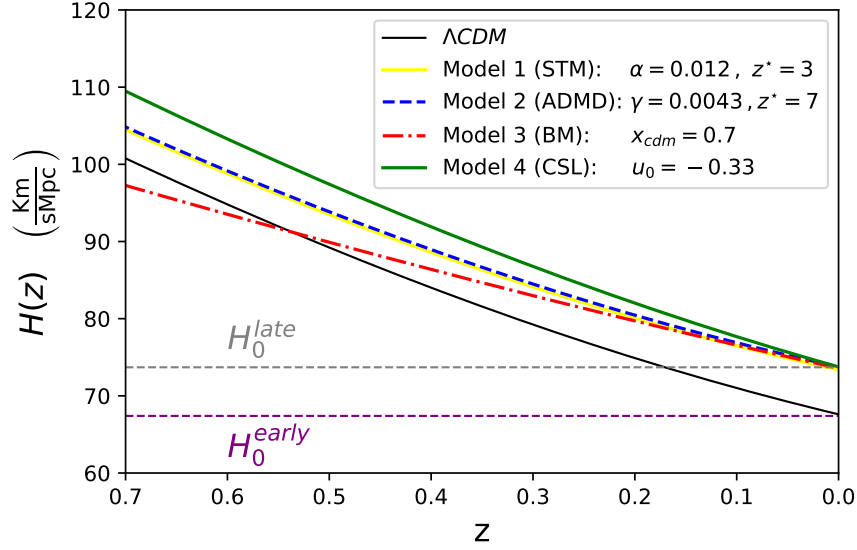


Figure 13: Cosmological evolution of the Hubble parameter $H(z)$ for all the diffusion models: STM (yellow), ADMD (blue), BM (red), and CSL (green). Solid black line shows the standard evolution without diffusion, i.e., the diffusion parameters set to zero. Horizontal dashed lines indicate the value of H_0 inferred from CMB (purple) and local observations (gray), whose values are respectively given by $H_0^{early} \simeq 68 \text{ km s}^{-1} \text{ Mpc}^{-1}$ and $H_0^{late} \simeq 73 \text{ km s}^{-1} \text{ Mpc}^{-1}$.

Therefore, from the numerical solutions that we have obtained, the four diffusion models studied seem to be good candidates to solve the tension in the value of H_0 . Focused on an analysis for the late time Universe, this was already shown for model 1 (STM) and model 2 (ADMD) in [58], where the authors explore the parameter space in order to find the possible combinations of the diffusion parameters such that $H_0^{early} \rightarrow H_0^{late}$, although no direct tests with observations are made. On the other hand, the authors in [59] studied models 3 and 4 (BM and CSL respectively), at late times as well. Particularly, in their study they analyze by parts each model depending on the contribution of the dark energy component: for the BM, they consider the cases in which 1) $\Omega_{0,\Lambda} = 0$, 2) $\Omega_{0,\Lambda} = 1$, 3) $0 < \Omega_{0,\Lambda} < 1$, and 4) $\Omega_{0,\Lambda} < 0$. For the CSL model, the cases that the authors analyze are 1) $\Omega_{0,\Lambda} > \Omega_{0,\xi}$, 2) $\Omega_{0,\Lambda} < \Omega_{0,\xi}$, and 3) $\Omega_{0,\Lambda} = \Omega_{0,\xi}$, where $\Omega_{0,\xi} \equiv \xi_{CSL}^2 / (9H_0^2)$. The authors include statistical analysis, but only considering local observations, such as Observational Hubble Data (OHD) used in [119], and supernovae (SNe Ia) [120].

We want to emphasise that it is crucial for any model trying to solve the H_0 tension to consider the radiation component of the Universe, since it plays an important role in the physics of the last scattering surface, specifically its contribution in the sound speed of the photon-baryon acoustic wave. In particular for models as those studied here, easing the H_0 tension should translate in the case in which CMB data are consistent with late time observations. This important part of the analysis is lacking in the previous works mentioned above, and it is the step further we are giving in this work in order to study the true viability of these models. We do not separate the analysis by cases, or restrict the diffusion models to low redshifts, but rather we contemplate all the cosmological evolution considering all the matter components present in the Universe.

Let us summarize the results obtained in this Section as follows: assuming that the values of the cosmological parameters are those inferred from CMB observations, in Figure 13 it is shown that, with the cosmological field equations obtained

from UG, it is possible to obtain a value of H_0 consistent with local observations by the means of diffusion processes between cold dark matter and dark energy in the form of a variable cosmological "constant". This is so, of course, for particular choices of the diffusion parameters. A statistical analysis have to be performed in order to infer the most likely values of such parameters in the light of current data taken from several astrophysical and cosmological observations.

3 Statistical analysis

In the previous Section, we have shown that diffusion processes in UG can ease the current tension on the H_0 parameter. Specifically, at the level of the numerical solutions for the background dynamics, the parameters of each diffusion model allow to have a consistent match between the H_0 inferred from CMB with that of local observations. It is crucial then, to analyze the viability of these models in the light of cosmological observations. Particularly, we want to constraint the diffusion parameters from models 1, 2, 3, and 4 with data from CMB observations. If these diffusion models ease the H_0 tension, then CMB data should allow values for α and z_* (for model 1), γ and z^* (for model 2), x_{cdm} (for model 3), and ξ_{CSL} (for model 4) such that the value of H_0 inferred by CMB coincides with that of local observations.

3.1 Constraints with CMB data set

Since we are focused on the background evolution, we will use the *Planck Compressed 2018* (PC2018) data [121], instead of the full Planck 2018 likelihoods. Such compressed version of the CMB data have been probed to be as useful as the full version, to constraint not only the standard Λ CDM model, but also alternative models of dark energy, such as ω CDM, CPL model, interacting dark energy, early dark energy, and all those models dubbed as *smooth dark energy*, which are models phenomenologically similar to a cosmological constant [122, 123, 124, 125, 126, 127, 128]. In our case, even when the gravitational theory is Unimodular Gravity, we have shown that the cosmological scenario is basically that of General Relativity with a non-gravitational interaction between the dark sector components. Particularly, we still have a cosmological "constant" which only changes its current value. Therefore, we can safely use PC2018 data to constraint the diffusion parameters.

The two main physical quantities to use in order to constraint cosmological models with PC2018 data are the acoustic scale l_A , which characterize the CMB temperature power spectrum in the transverse direction (and therefore leading to variations of the peak spacing), and the shift parameter R , which affects the CMB temperature spectrum in the line-of-sight direction (and therefore affecting the heights of the peaks),

$$l_A = (1 + z_*)\pi \frac{D_A(z_*)}{r_s(z_*)}, \quad R = (1 + z_*) \frac{\Omega_{0,m}^{1/2} H_0}{c} D_A(z_*), \quad (22)$$

where z_* is the value of the redshift when photons decouple from baryons ($z_* \simeq 10^3$), c is the speed of light, and r_s and D_A are the comoving sound horizon and the angular diameter distance respectively,

$$r_s(z) = \frac{1}{H_0} \int_z^\infty \frac{c_s(z') dz'}{E(z')}, \quad \text{with} \quad c_s(z) = c \left[3 \left(1 + \frac{3\Omega_b}{4\Omega_r(1+z)} \right) \right]^{-1/2}, \quad (23a)$$

$$D_A(z) = \frac{c}{H_0(1+z)} \int_0^z \frac{dz'}{E(z')}, \quad \text{for} \quad \Omega_k = 0, \quad (23b)$$

where $c_s(z)$ is the sound speed of the photon-baryon acoustic wave. Additionally, the physical baryon energy density parameter $\Omega_b h^2$ with $h = H_0/100$, and the scalar spectral index n_s are included in the PC2018 likelihood as well. It can be seen that the diffusion parameters enter through $E(z)$ given by Eq. (18c), (19c), (20c), (21e), for model 1, 2, 3, and 4 respectively, in the integrands shown in Eq. (23). Here it is evident the importance to have the radiation component in the analysis, since we have to evaluate integrals on z_* in order to compute l_A and R (see Eq. (22)).

The parameter space of interest for each diffusion model will be spanned by

$$\Theta_1 = \{ \Omega_b h^2, \Omega_{cdm} h^2, H_0, \alpha, z_1^* \}, \quad (24a)$$

$$\Theta_2 = \{ \Omega_b h^2, \Omega_{cdm} h^2, H_0, \gamma, z_2^* \}, \quad (24b)$$

$$\Theta_3 = \{ \Omega_b h^2, \Omega_{cdm} h^2, H_0, x_{cdm} \}, \quad (24c)$$

$$\Theta_4 = \{ \Omega_b h^2, \Omega_{cdm} h^2, H_0, \xi_{CSL} \}, \quad (24d)$$

This will explicitly show whether the diffusion parameters can take non-null values consistent with CMB data, and simultaneously solving the H_0 tension. The (logarithmic) likelihood function $\log \mathcal{L}(\Theta)$ is given by

$$\log \mathcal{L}_{\text{CMB}}(\Theta) = -\frac{1}{2} [\vec{\mu}_{\text{CMB}} - \vec{\mu}(\Theta)]^T \mathbf{C}_{\text{CMB}}^{-1} [\vec{\mu}_{\text{CMB}} - \vec{\mu}(\Theta)], \quad (25)$$

where $\mathbf{C}_{\text{CMB}}^{-1}$ is the inverse covariance matrix of the CMB observation, $\vec{\mu}_{\text{CMB}} = (R^{\text{CMB}}, l_A^{\text{CMB}}, (\Omega_b h^2)^{\text{CMB}}, n_s^{\text{CMB}})$ is the vector of CMB observations, and $\vec{\mu}(\Theta_i) = (R(\Theta_i), l_A(\Theta_i), \Omega_b h^2, n_s)$ is the vector of their corresponding theoretical values according to the diffusion models $i = 1, 2, 3, 4$.

To compute the posteriors probabilities for each of the diffusion models, we use the software MONTE PYTHON [129]. We have considered flat priors, since they are the most conservatives to use when there is not previous knowledge about the parameters to analyze, as is the case for the diffusion models. As can be seen in Table 1, we have chosen the mean of the diffusion parameters to be those agreeing with Λ CDM, but with broad priors. For instance, the characteristic redshift z_1^* (z_2^*) for Model 1 (Model 2) is such that, the diffusion process can take place at any moment between the last scattering surface ($z \simeq 1100$) and the present day ($z = 0$). The prior for H_0 is such that it contains the two preferred and different mean values reported by cosmological and local observations. On the other hand, the prior for the physical baryon density parameter $\Omega_b h^2$ was established such that $0 \leq \Omega_b \leq 1$, and according to the prior for H_0 mentioned above $0.65 \leq h \leq 0.75$. The prior for the CDM parameter $\Omega_{\text{cdm}} h^2$ was established in the same way.

model	parameter	mean	min prior	max prior	Std. Dev.
Λ CDM	$\Omega_b h^2$	0.0224	0	0.5625	0.015
	$\Omega_{\text{cdm}} h^2$	0.120	0	0.5625	0.0013
	H_0	70	65	75	0.01
Model 1	α	0	-1	1	0.005
	z_1^*	0	0	1100	0.005
Model 2	γ	0	-10	10	0.005
	z_2^*	0	0	1100	0.005
Model 3	x_{cdm}	0	-0.01	0.05	0.001
Model 4	u_0	0	-10	10	0.005

Table 1: Input for the parameters of each diffusion model to generate the MCMC. Each diffusion model also has the same input for the Λ CDM parameters.

When running the chains, we have monitored the convergence with the Gelman–Rubin criterion [130], by considering $R - 1 < 0.05$. Figure 14 shows the posteriors for the parameters of Model 1 (top left, orange), 2 (top right, blue), 3 (bottom left, red), and 4 (bottom right, green). The posteriors for the Λ CDM parameters (gray) are shown for comparison.

As general features shared by all the diffusion models, we observe from the posteriors of the standard Λ CDM parameters that 1) the amount of baryonic matter $\Omega_b h^2$ remains unchanged, 2) the amount of cold dark matter $\Omega_{\text{cdm}} h^2$ gets a broader range of values, and since it is anticorrelated with the Hubble parameter², 3) H_0 is weakly constrained, and its posterior gets “stretched”. This is not the ideal way to ease the H_0 tension, in the sense that it would be desirable CMB data to be consistent with local observations by shifting the mean value of H_0 from H_0^{early} to H_0^{late} .

In the case of the diffusion parameters from models 1 and 2 we have,

$$\text{Model 1 (STM)} : \quad \alpha = -0.0202_{-0.0152}^{+0.0317}, \quad z_1^* = 1.58_{-1.58}^{+0.256}. \quad (26a)$$

$$\text{Model 2 (ADMD)} : \quad \gamma = -0.633_{-0.728}^{+1.67}, \quad z_2^* = 0.247_{-0.247}^{+0.0269}. \quad (26b)$$

Whereas in [58] the diffusion parameters α and γ are defined strictly positives, we are regarding their values to be constrained by observations, and in principle there is not restriction on the sign of these parameters. Moreover, if they have to be consistent with Λ CDM, it is convenient to consider a symmetric range around zero. This allow us to see that the most likely values for those parameters have negative mean values, with a standard deviation including α, γ equal to zero, where the Λ CDM model is recovered. On the other hand, the characteristic redshift is $z^* \geq 0$, since the energy transfer between CDM and Λ occurs at some time between the last scattering surface and the present day. Both models present a transfer of energy taking place at $z_1^* = 1.58$ for model 1, and $z_2^* = 0.247$ for model 2, which is consistent with a late time diffusion process. The novelty here is that we were able to infer such values through CMB observations, which requires to calculate the angular diameter distance D_A at $z_* \simeq 1100$ in order to compute the observables l_A and R (see Eq. (22) and Eq. (23b)),

$$D_A(z_*) = \frac{c}{H_0(1+z_*)} \int_0^{z_*} \frac{dz'}{E(z')} = \frac{c}{H_0(1+z_*)} \left[\int_0^{z_i^*} \frac{dz'}{E_i(z')} + \int_{z_i^*}^{z_*} \frac{dz'}{E_{\Lambda\text{CDM}}(z')} \right], \quad (27)$$

²While this anticorrelation is true in the Λ CDM case, strictly speaking, the anticorrelation between $\Omega_{\text{cdm}} h^2$ and H_0 occurs for the diffusion models 1, 2, and 4. In the case of model 3 the $\{\Omega_{\text{cdm}} h^2, H_0\}$ -plane present a banana-shaped posterior, and the anticorrelation occurs only for the region corresponding with positive values of x_{cdm} .

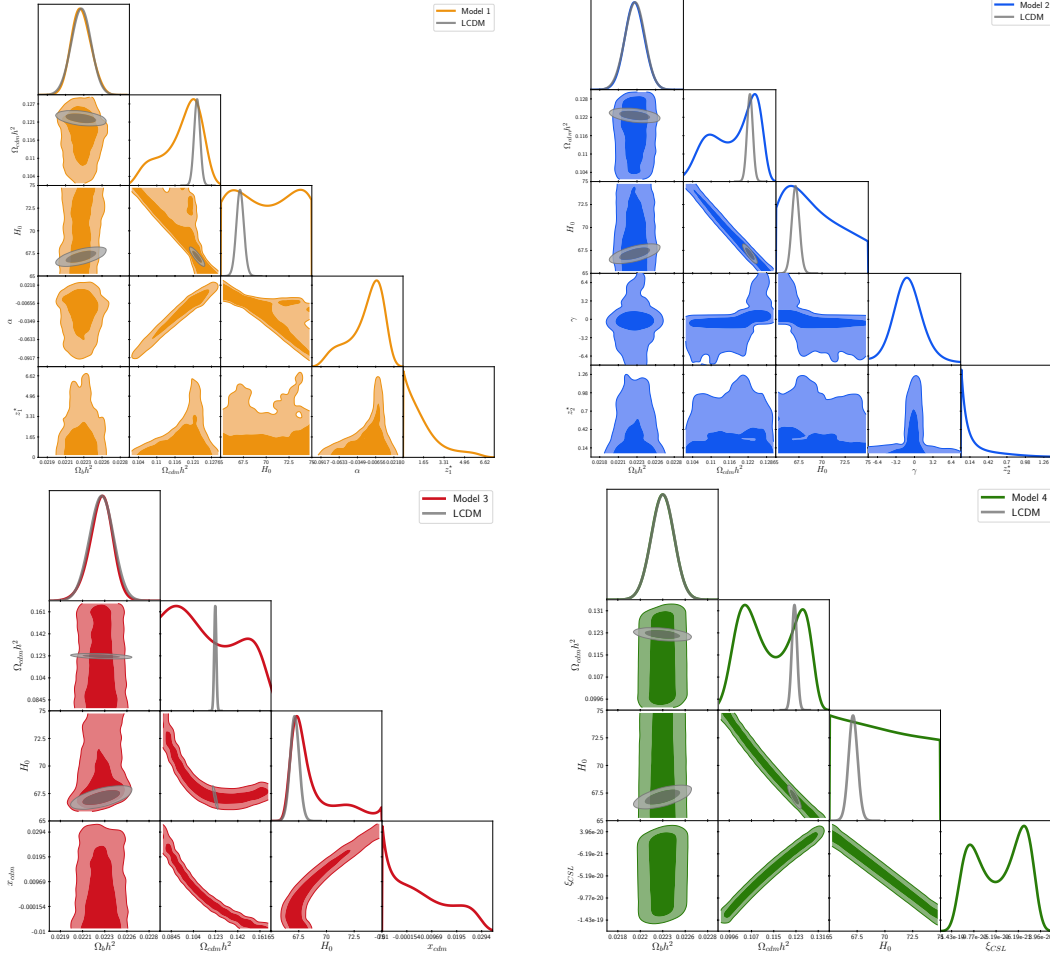


Figure 14: Posterior probability distributions considering CMB data only, for all diffusion models under study: Sudden Transfer model (top right, orange), Anomalous Decay of the Matter Density model (top right, blue), Barotropic model (bottom left, red), and Continuous Spontaneous Localization model (bottom right, green). We have included the posteriors for the Λ CDM parameters as well (gray).

where $E_i(z)$ stands for the normalized Friedmann equations (18c), (19c) according to the models $i = 1, 2$ respectively, with z_i^* the corresponding characteristic redshift, and $E_{\Lambda\text{CDM}}(z)$ for the standard Λ CDM case. The first integral within the square brackets quantify the modification induced by the diffusion process.

In the case of model 3, the diffusion parameter presents an upper bound at $x_{\text{cdm}} \simeq 0.03$. This allows to the CDM energy density parameter to have a broader range of values. However, the constraint on H_0 is not as weak as that imposed on such parameter by the other diffusion models. The parameter ξ_{CSL} of model 4 presents a posterior with two peaks located at $\xi_{\text{CSL}} \simeq (-1.09 \times 10^{-19}, 5.26 \times 10^{-21}) \text{ s}^{-1}$, which constitute the most likely values for such parameter. These peaks on ξ_{CSL} induce a bimodal posterior in the CDM density parameter whose peaks are located at $\Omega_{\text{cdm}} h^2 \simeq (0.105, 0.125)$. While one of the peaks is approximately consistent with the amount of CDM according to the Λ CDM model, the second peak is located at less CDM contribution, which lead to higher values of H_0 .

Therefore, whereas for Λ CDM we obtained the expected values inferred from CMB for $\Omega_b h^2$, $\Omega_{\text{cdm}} h^2$, and H_0 given by

$$\Omega_b h^2 = 0.0223_{-0.000137}^{+0.000136}, \quad \Omega_{\text{cdm}} h^2 = 0.122_{-0.00095}^{+0.000968}, \quad H_0 = 67.1_{-0.438}^{+0.427} \text{ km s}^{-1} \text{ Mpc}^{-1}, \quad (28)$$

the diffusion parameters allow to increase the range of values that CDM energy density and H_0 usually have within the Λ CDM model according to CMB data. In particular, H_0 is weakly constrained and it can take values from H_0^{early} to H_0^{late} while being in agreement with CMB observations. However, and as we mentioned above, this is not the ideal way to ease the H_0 tension, in the sense that the mean value of H_0 should shift from H_0^{early} to H_0^{late} , if it is the case

that these models solve the tension successfully. The latter can be explored by adding new information to the analysis, new data sets that help to break some degeneracies between the parameters.

3.2 Constraints with CMB + Late time data set

So far we have obtained that the diffusion models presented here seem to ease the H_0 tension, but in such a way that, instead of an effective shift of the mean value, the constraint on H_0 is weaker than in the Λ CDM case due to the presence of the diffusion parameters. Therefore, let us now include observations from the late Universe to study whether the diffusion models are in agreement with $H_0 = H_0^{\text{late}}$ under the combined analysis CMB+SH0ES+H0LICOW+SNe Ia.

Besides the cosmological observation from the CMB ($z_* \sim 1100$), we now include some local observations to the analysis: **Pantheon**, light-curve from 1048 supernovae (SNe Ia) within the redshift range $0.01 < z < 2.26$ [120]. **H0LICOW**³, time-delay distances of 6 lensed quasars at redshifts $z = 0.654, 1.394, 1.662, 1.693, 1.722, 1.789$ [132, 133, 134, 135, 136, 137, 138, 96]. **SH0ES**, H_0 measurement from Cepheids in the Large Magellanic Cloud ($d \sim 50\text{kpc}$) [92].

The current constraints on H_0 from Planck, SH0ES, and H0LICOW can be seen in the next Figure⁴, where it is also included the H_0 value for the combination of these two late Universe observations, as well as the corresponding tension T_{H_0} calculated according to the estimator [139]

$$T_{H_0} = \frac{|\mu_{\text{early}} - \mu_{\text{late}}|}{\sqrt{\sigma_{\text{early}}^2 + \sigma_{\text{late}}^2}}, \quad (29)$$

where μ_{early} (μ_{late}) is the mean value of H_0^{early} (H_0^{late}), and σ their corresponding standard deviation.

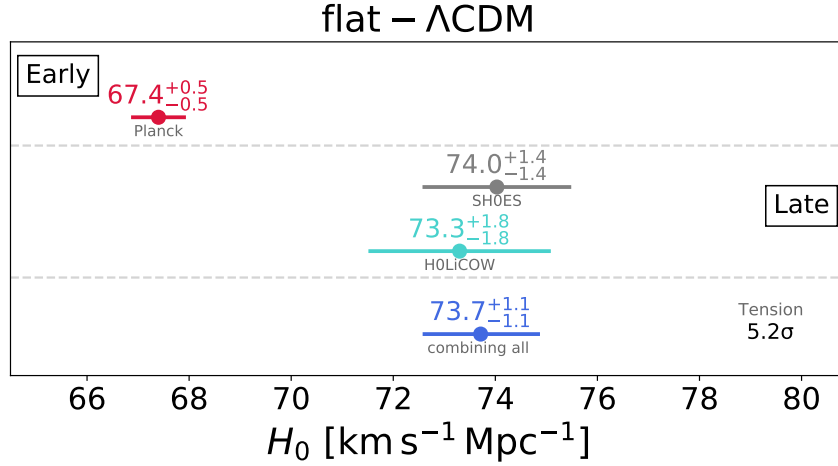


Figure 15: Reduced version of Figure 1 considering the observations we will use. Constraints on H_0 from early (top) and late (middle) time observations. It is also shown the value of H_0 inferred from the combination of the two late Universe observations considered in this work (bottom). There is a tension of 5.2σ between the value of H_0 inferred from early Universe (Planck) and that obtained from late time observations (SH0ES+H0LICOW). Pantheon is not shown since it alone does not constraint H_0 . See text for more details.

Supernovae (SNe Ia)

Observations from the luminosity of SNe Ia allow to estimate their distances. The model for the observed distance modulus μ_{SNe} is the following [120],

$$\mu_{SNe} = m_B^* - M, \quad \text{with} \quad m_B^* = m_B + \tilde{\alpha}X_1 - \beta C + \Delta_M + \Delta_B, \quad (30a)$$

³For the MONTE PYTHON implementation of the H0LICOW likelihoods see [here](#) [131].

⁴For an editable version of Figure 1, like the one presented in Figure 15 see [here](#) [99].

where m_B^* corresponds to the corrected apparent peak magnitude, X_1 describes the time stretching of the light-curve, C stands for the supernova color at maximum brightness, and $\tilde{\alpha}, \beta, M, \Delta_M, \Delta_B$ are nuisance parameters⁵ [140, 141, 142]. On the other hand, the distance modulus which relies on the cosmological model is

$$\mu(z) = 5 \log \left[\frac{d_L(z)}{10 \text{ pc}} \right], \quad \text{with} \quad d_L(z) = \frac{c(1+z)}{H_0} \int_0^z \frac{dz'}{E(z')}, \quad (30b)$$

where $d_L(z)$ is the luminosity distance. Then, the likelihood function will be,

$$\log \mathcal{L}_{\text{SNe}}(\Theta) = -\frac{1}{2} [\vec{\mu}_{\text{SNe}} - \vec{\mu}(\Theta)]^T \mathbf{C}_{\text{SNe}}^{-1} [\vec{\mu}_{\text{SNe}} - \vec{\mu}(\Theta)], \quad (30c)$$

where $\vec{\mu}_{\text{SNe}}$ and $\vec{\mu}(\Theta)$ are respectively given by Eq. (30a) and (30b) for each supernova, and \mathbf{C}_{SNe} is the covariance matrix.

It is important to mention that H_0 can not be constrained when using only SNe Ia because H_0 and the nuisance parameter M are strongly degenerated [120]. Thus, data from SNe Ia should be combined with other observations in order to constraint H_0 properly.

Quasars (QSR)

Strong gravitational lenses allow to measure distances through the time delay between the multiple images of the lensed source. The H_0 Lenses in COSMOGRAIL'S Wellspring (H0LICOW) program have measured the current value of the Hubble parameter from a joint analysis of six gravitationally lensed quasars with measured time delay.

The time delay of an image i in comparison with the no lensing case is [143],

$$t(\theta_i, \beta) = \frac{D_{\Delta t}}{c} \phi(\theta_i, \beta), \quad (31a)$$

where θ_i is the position of the lensed image of i , β is the source position, $D_{\Delta t}$ is the so-called *time-delay distance*, ϕ is the *Fermat potential*, and c is the speed of light. For a lens at redshift z_d and a source at redshift z_s , the time-delay distance is given by,

$$D_{\Delta t} = (1 + z_d) \frac{D_d D_s}{D_{ds}}, \quad (31b)$$

where D_d and D_s are the angular diameter distances to the lens and to the source respectively, whereas D_{ds} is the angular diameter distance between the lens and the source (see Eq. (23b)). By measuring the time delay between two images i and j , we have

$$\Delta t_{ij} = t(\theta_i, \beta) - t(\theta_j, \beta) = \frac{D_{\Delta t}}{c} \Delta \phi_{ij}. \quad (31c)$$

Once determined the Fermat potential (by modeling the lens mass distribution), and with Δt measured, it is possible to infer the value of the time-delay distance $D_{\Delta t}$. Thus, the likelihood function is,

$$\log \mathcal{L}_{\text{QSR}}(\Theta) = -\frac{1}{2} [\vec{\mu}_{\text{QSR}} - \vec{\mu}(\Theta)]^T \mathbf{C}_{\text{QSR}}^{-1} [\vec{\mu}_{\text{QSR}} - \vec{\mu}(\Theta)], \quad (31d)$$

where $\vec{\mu}(\Theta)$ and $\vec{\mu}_{\text{QSR}}$ are respectively given by Eq. (31b) and (31c) for each lensed quasar, and \mathbf{C}_{QSR} is the covariance matrix.

Cepheids (CPH)

Cepheids provide a way to measure distances through the period-luminosity relation characterizing them. Particularly, from 70 long-period Cepheids observed by the Hubble Space Telescope (HST) in the Large Magellanic Cloud, the Supernova H_0 for the Equation of State (SH0ES) collaboration have determined the current value of the Hubble parameter $H_0^{\text{CPH}} = 74.03 \pm 1.42 \text{ km/s/Mpc}$ [92]. The likelihood function is then given by,

$$\log \mathcal{L}_{\text{CPH}}(H_0) = -\frac{1}{2} \frac{[H_0^{\text{CPH}} - H_0]^2}{\sigma_{\text{CPH}}^2}. \quad (32)$$

The likelihood function associated to these late Universe observations is given by,

$$\log \mathcal{L}_{\text{Late}}(\Theta) = \log \mathcal{L}_{\text{SNe}}(\Theta) + \log \mathcal{L}_{\text{QSR}}(\Theta) + \log \mathcal{L}_{\text{CPH}}(H_0), \quad (33)$$

⁵We have used a tilde on the nuisance parameter $\tilde{\alpha}$ to avoid confusions with the diffusion parameter α from Model 1 STM.

and finally, the total likelihood function will be the following,

$$\log \mathcal{L}_{tot}(\Theta) = \log \mathcal{L}_{CMB}(\Theta) + \log \mathcal{L}_{Late}(\Theta). \quad (34)$$

Considering the same initial mean values, priors, and standard deviations shown in Table 1, Figure 16 shows the posteriors for each diffusion model as well as those for the Λ CDM model. It can be observed that the posteriors for the Λ CDM parameters (gray) do not change considerably with respect to the posteriors obtained in the previous analysis when only CMB data were considered (see Eq. (28)). This time we have,

$$\Omega_b h^2 = 0.0225^{+0.000134}_{-0.000132}, \quad \Omega_{cdm} h^2 = 0.121^{+0.000877}_{-0.000887}, \quad H_0 = 67.9^{+0.399}_{-0.403} \text{ km s}^{-1} \text{ Mpc}^{-1}. \quad (35)$$

Particularly, the mean of H_0 slightly increases its value from 67.1 to 67.9 $\text{km s}^{-1} \text{ Mpc}^{-1}$ and, as expected from the Λ CDM model, the tension persists when this result is compared with the mean value of H_0 inferred from late time observations.

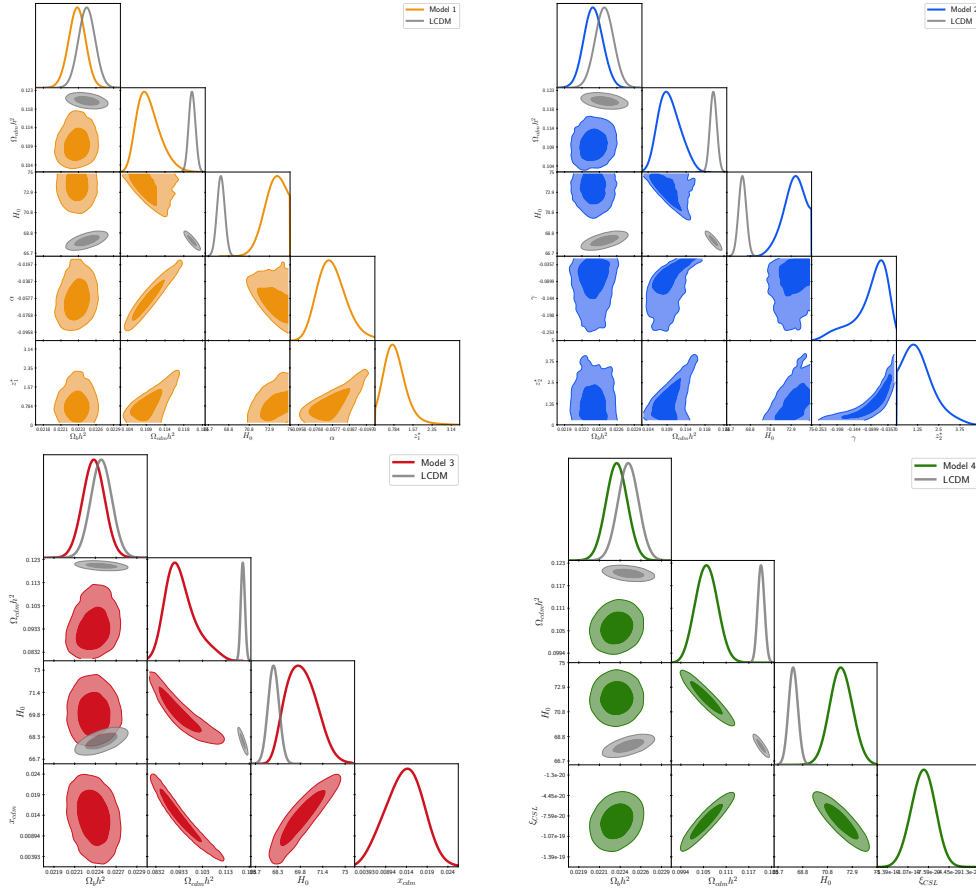


Figure 16: Posterior probability distributions considering CMB+SNe+QSR+CPH data for all diffusion models under study: Sudden Transfer model (top right, orange), Anomalous Decay of the Matter Density model (top right, blue), Barotropic model (bottom left, red), and Continuous Spontaneous Localization model (bottom right, green). We have included the posteriors for the Λ CDM parameters as well (gray).

With the aim of quantify how much the tension is eased in the case of the diffusion models, let us propose a similar estimator to that of Eq. (29),

$$\mathcal{T}_{H_0} \equiv \frac{|\mu_{comb} - \mu_{late}|}{\sqrt{\sigma_{comb}^2 + \sigma_{late}^2}}, \quad (36)$$

where μ_{comb} and σ_{comb} are respectively the mean and standard deviation of H_0 according to the combined analysis CMB+SNe+QSR+CPH, whereas μ_{late} and σ_{late} are the mean and standard deviation of H_0 from the SH0ES and

H0LICOW combined observations given by $H_0 = 73.7^{+1.1}_{-1.1} \text{km s}^{-1} \text{Mpc}^{-1}$ (see bottom panel of Figure 15)⁶. In particular, we define σ_{comb} as the following mean value $\sigma_{comb} \equiv (\sigma_{comb}^+ + \sigma_{comb}^-)/2$ to incorporate the case of an asymmetric standard deviation.

It is important to recall that when only CMB data are considered, the posteriors of H_0 for the diffusion models are weakly constrained, and there is not a mean value with an associated standard deviation that can be used to compare with local observations. As discussed in the previous Section, the presence of new parameters allows a broad range of values for the current Hubble parameter. On the other hand, since the value of H_0 does not change considerably between the CMB analysis and that of CMB+SNe+QSR+CPH, the results from the latter give approximately the same tension as that obtained from the former. This motivate us to propose Eq. (36). Table 2 shows the mean and 1- σ confidence level for the Λ CDM and diffusion parameters. The tension \mathcal{T}_{H_0} for each model is shown as well.

model	parameter	mean $^{+1\sigma}_{-1\sigma}$	\mathcal{T}_{H_0}
Λ CDM	$\Omega_b h^2$	$0.0225^{+0.000134}_{-0.000132}$...
	$\Omega_{cdm} h^2$	$0.121^{+0.000877}_{-0.000887}$...
	H_0	$67.9^{+0.399}_{-0.403}$	5.0σ
Model 1	$\Omega_b h^2$	$0.0223^{+0.000135}_{-0.000135}$...
	$\Omega_{cdm} h^2$	$0.109^{+0.00233}_{-0.00356}$...
	H_0	$73.4^{+1.46}_{-0.588}$	0.2σ
	α	$-0.0582^{+0.0134}_{-0.0182}$...
	z_1^*	$0.842^{+0.318}_{-0.547}$...
Model 2	$\Omega_b h^2$	$0.0223^{+0.000134}_{-0.000139}$...
	$\Omega_{cdm} h^2$	$0.109^{+0.00254}_{-0.0032}$...
	H_0	$73.2^{+1.38}_{-0.86}$	0.3σ
	γ	$-0.089^{+0.0672}_{-0.0212}$...
	z_2^*	$1.41^{+0.414}_{-1.13}$...
Model 3	$\Omega_b h^2$	$0.0224^{+0.000138}_{-0.000139}$...
	$\Omega_{cdm} h^2$	$0.094^{+0.00467}_{-0.00784}$...
	H_0	$70^{+0.949}_{-1.17}$	2.4σ
	x_{cdm}	$0.0135^{+0.00475}_{-0.00436}$...
Model 4	$\Omega_b h^2$	$0.0223^{+0.000136}_{-0.000138}$...
	$\Omega_{cdm} h^2$	$0.106^{+0.00284}_{-0.00301}$...
	H_0	$72^{+0.951}_{-0.969}$	1.1σ
	ξ_{CSL}	$(-8.4^{+1.86}_{-1.82}) \times 10^{-20}$...

Table 2: Mean values and their corresponding 1 σ confidence level for the parameters of each diffusion model, as well as for the Λ CDM parameters. The units of H_0 and ξ_{CSL} are given respectively by $\text{km s}^{-1} \text{Mpc}^{-1}$ and s^{-1} . The last column indicates the tension \mathcal{T}_{H_0} according to Eq. (36). See the text for more details.

We want to end this Section by highlighting the following: having included local observations in the analysis led to specific and well-defined values of the diffusion parameters. In particular, the amount of CDM and H_0 get precise values, opposite to the case in which only CMB data was used. The amount of total matter $(\Omega_b + \Omega_{cdm}) h^2$ predicted by the diffusion models is less than the Λ CDM case, which translates in a higher value for H_0 . This indicates that the diffusion models are, effectively, good candidates to alleviate the H_0 tension. In this sense, our statistical analysis verifies what we have obtained numerically in the previous Section: within the framework of Unimodular Gravity, the non-gravitational interaction between the dark sector components through diffusion processes, leads to an inferred value of H_0 consistent with local observation when constraining the diffusion parameters with CMB data and CMB+local observations.

⁶The presence of SNe Ia in the combined analysis we have made does not affect the results obtained from the estimator (36). Since SH0ES and H0LICOW impose the late time constraint on H_0 , once combined, SNe Ia data are in agreement with such constraints. Thus, we do not expect a substantial change on the combined SH0ES+H0LICOW value $H_0^{late} = 73.7^{+1.1}_{-1.1} \text{km s}^{-1} \text{Mpc}^{-1}$ due to SNe Ia.

4 Discussion and final remarks

Whereas the main ingredient responsible of the dynamics of the late Universe remains unknown, the best model to explain the current accelerated expansion is given by the cosmological constant in the Einstein field equations. Nonetheless, the origin of such constant is still unknown, although there are several theoretical proposals trying to understand its nature. Unimodular Gravity offers an explanation of the origin of the cosmological constant: it arises as an integration constant once volume-preserving diffeomorphisms are considered in the Einstein–Hilbert action. The dynamics of the spacetime metric is governed by the trace-free version of the Einstein field equations and, as a direct consequence, the energy–momentum tensor is not conserved once the Bianchi identities are applied. The non-conservation of the energy–momentum tensor allows matter components to interact with each other non-gravitationally. Since the physics of the standard model of particles is very well understood, we have assumed the non-gravitational interaction to be possible only between the dark sector components, which are given by a cold dark matter fluid ρ_{cdm} and an effective cosmological constant with dependence on the cosmic time $\Lambda(t)$. To describe the interaction between ρ_{cdm} and $\Lambda(t)$, we have considered phenomenological models previously studied in [58, 59], where the authors propose diffusion processes as the mechanism for the energy transfer from one dark component to the other.

In general, models with non-gravitational interactions in the dark sector have been studied with emphasis in the H_0 tension, this is, the current discrepancy between the value of the Hubble parameter at present day inferred from early Universe, and that inferred from local observations. The authors in [58, 59] have also analyzed the possibility of ease such tension through diffusion processes between ρ_{cdm} and $\Lambda(t)$ in UG. However, their analysis have been restricted to the dynamics of the late Universe which, although some hints about the viability of these models can be obtained, a more suitable analysis must involve physics of the early Universe, in particular the radiation component has to be included in the cosmological evolution. This is important because any model addressing the H_0 tension must be tested not only with late time observations, but with CMB data as well. For the latter it is mandatory to evaluate the model at high redshifts, in particular at the moment of photon–baryon decoupling occurring at $z_* \simeq 1100$. Thus, we have implemented each of the diffusion models studied in the works mentioned before, in a more realistic cosmological scenario, where the background evolution includes the presence of photons and ultra-relativistic neutrinos as the components of radiation in the Universe.

Considering a spatially-flat FRW line element, we have solved the UG field equations, from very deep in the radiation domination era (initial redshift $z(t_i) = 10^{14}$) to the present day ($z(t_0) = 0$), with special interest in the cosmological evolution of the energy density parameters Ω_i where $i = b, \gamma, \nu, cdm, \Lambda$ stands for baryons, photons, neutrinos, cold dark matter, and cosmological constant respectively. We explicitly showed how the diffusion process takes place between Ω_{cdm} and Ω_Λ for each of the four diffusion models studied: Sudden Transfer Model (STM) and Anomalous Decay of the Matter Density (ADMD) from [58], and Barotropic Model (BM) and Continuous Spontaneous Localization (CSL) from [59], for which we have obtained the corresponding modified Friedmann equation (18c), (19c), (20c), and (21e). For the BM and CSL model, we have implemented a different approach to that of the authors in [59]: instead of separating the analysis by cases depending on the contribution of the cosmological constant energy density, we have solved the full set of background equations for all the cosmological evolution considering the modification on $H(z)$ due to the diffusion models. In particular, this was not direct to do for the CSL model, which expression for the Friedmann equation involves an integro-differential equation for $z(t)$. In appendix A we show the method we have used to address this difficulty, which allowed us to write in a closed form the modification in $H(z)$ due to the CSL diffusion model. It was crucial to have the expression of the modified Friedmann equation for each diffusion model, since later in the statistical analysis, $H(z)$ enters in the angular diameter distance D_A that is needed to compute the observables from CMB (Eq. (22)) and Quasars (Eq. (31b)), as well as in the distance modulus μ through the luminosity distance d_L for SNe Ia (Eq. (30b)).

We explored the influence of the diffusion parameters on the dynamics of the dark sector, as well as how these parameters modify the current amount of the dark components energy densities. The magnitude and sign of the diffusion parameters set the contribution of both, Ω_{cdm} and Ω_Λ , and thus, the Hubble parameter at present day change its value as well. In particular, when considering that the values of each Ω_i and H_0 are those reported by CMB observations (and then $H_0 = H_0^{early} \simeq 67 \text{ km s}^{-1} \text{ Mpc}^{-1}$), we have shown that it is possible to find values of the diffusion parameters such that the diffusion models lead to a Hubble parameter at $z = 0$ consistent with the value obtained from data of the local Universe (i.e., $H_0 = H_0^{late} \simeq 73 \text{ km s}^{-1} \text{ Mpc}^{-1}$). Therefore, at the level of the numerical solutions, all the diffusion models ease the H_0 tension. Nonetheless, to truly test these models and to analyze properly their viability as compelling candidates to solve the discrepancy on the measurement of the current value of the Hubble parameter, it is mandatory a statistical analysis. While such analysis was not performed in [58], the authors in [59] constraint the BM and CSL model by using data from late time observations (Observational Hubble Data (OHD) and supernovae (SNe Ia)). As we mentioned before, to establish a proper comparison between the predictions of the diffusion models in what the H_0

tension is concerned, not only data set from local observations have to be considered, but from the early Universe as well. We have done this by using the Planck Compressed 2018 data.

Since the diffusion models predict less amount of matter in order to rise the value of H_0 , we have let to vary both the physical energy density for baryons $\Omega_b h^2$ and CDM $\Omega_{cdm} h^2$, considering the broadest priors possible. Besides, the prior for H_0 included the observed mean values from both, early and late time Universe. In the case of the diffusion parameters, we also considered the broadest priors possible. In fact, by setting the more broadest priors have costed to expend more time for the chains to converge when exploring the parameter space. This is so because the new parameters from the diffusion models induce a longer anticorrelation between $\Omega_{cdm} h^2$ and H_0 , and more possible combinations of such parameters are allowed by the observations in comparison with the Λ CDM case. When considering only CMB observations, the additional parameters from the diffusion models allow to ease the tension on H_0 , for which weaker constraints are imposed. In fact, the CDM energy density parameter Ω_{cdm} is weakly constrained as well, and given that the diffusion parameters lead to lower values of Ω_{cdm} , this translates to higher values of H_0 . Thus, the posteriors for H_0 get a broader range of values, which includes those inferred from both early and late time Universe (see Figure 14). It is when local observations are included into the analysis that an actual shift on the mean value of H_0 occurs (see Figure 16).

In the case of the model 1 (STM), negative values of the diffusion parameter α are preferred by observations. This is not the case in [58] where such parameter is defined such that $0 < \alpha < 1$, and the parameter space is restricted for positive α only. However, our result is not in contradiction with the prediction of the model: the contribution of matter today will be less than the predicted by Λ CDM. In fact, this is a prediction of all the diffusion models studied, as can be seen in Figure 16 where both $\Omega_b h^2$ and $\Omega_{cdm} h^2$ for the STM (red), ADMD (blue), BM (red), and CSL (green) are shifted to the left in comparison with the Λ CDM case (gray). Since the amount of baryons is a well-measured quantity, the shift is less than 1%, whereas for CDM the differences are approximately 9.9% for STM and ADMD, 22.3% for BM, and 12.4% for CSL. For the diffusion parameter γ from model 2 (ADMD), we observe that a negative value is preferred as well. The characteristic redshift z^* for models 1 and 2 are constrained to low redshifts, this is, the diffusion processes described by these models occur in the late Universe. Such constraints were obtained under the assumption that the diffusion process could take place at any time between the last scattering surface and the present day, which was important to consider since, according to the analysis of the parameter space carried out in [58], larger values of z^* lead to values of α and γ such that the Λ CDM case is recovered, i.e., for $z^* \gg 1$, $\alpha, \gamma \rightarrow 0$ (see Figures 3 and 6 from [58]).

The constraint we have obtained on the diffusion parameter x_{cdm} from model 3 (BM) is in agreement with that reported in [59] for the case in which the authors infer the value of x_{cdm} from OHD and SNe Ia independently ($x_{cdm} = 0.027^{+0.046}_{-0.045}$, $0.041^{+0.310}_{-0.194}$ for OHD and SNe Ia respectively). In the joint analysis OHD–SNe Ia, the constraint obtained in [59] is given by $x_{cdm} = 0.054^{+0.035}_{-0.032}$, which is larger than the inferred value in our analysis. Nonetheless, as can be compared from the reported values in [59] shown above and our results, our uncertainties for x_{cdm} are smaller (see Model 3 in Table 2). In the case of H_0 , our result is consistent with that of the authors, at least when compared with their analysis for OHD and OHD+SNe Ia. As we mentioned in Section 3.2, the Pantheon data set alone can not be used to constraint the H_0 since it is degenerated with M [120]. In order to have a H_0 measurement only from SNe Ia, we have noticed that in [59] the authors have rewritten the supernovae likelihood only as a function of the redshift and the cosmological parameters, and no nuisance parameters are present (see Eq.55 in [59]). This gives a value of $H_0 = 73.2^{+1.7}_{-1.7}$, which is larger than the inferred value of H_0 in our analysis for model 3. In the case of model 4 (CSL), our inferred value for ξ_{CSL} is incompatible with the constraints found in [61, 144, 59], where positive values for such parameter are inferred, whereas from our analysis we have obtained that $\xi_{CSL} < 0$. Nonetheless, let us to pinpoint out the following aspects to be regarded: in the works mentioned above, the non-gravitational interaction includes ordinary matter, since the authors consider energy transfer between the cosmological constant and the total matter content ρ_m . It has to be recalled that in our case, the violation of the energy–momentum tensor is produced only through the components of the dark sector. On the other hand, as discussed in [61] the sign of ξ_{CSL} can be negative, which implies an endothermic evolution. The latter scenario can be obtained, for instance, from approaches to quantum gravity such as *causal set* [145, 146],

With the aim of quantify how much these diffusion models ease the tension on H_0 , we proposed an estimator \mathcal{T}_{H_0} to compute the differences between our combined analysis CMB+SNe+QSR+CPH and local observations from SH0ES and H0LICOW (see Eq. (36)). The model 1 (STM) is the one reducing more the tension with a difference of 0.2σ , whereas model 3 (BM) gives the larger difference by easing the tension at 2.4σ . These results indicate that diffusion models in UG are viable theoretical proposals to solve the H_0 tension.

It will be interesting to explore the cosmological perturbations for the diffusion models studied. Previous works have made some contributions in this direction, although imposing by hand the conservation of the energy–momentum tensor, which as we have shown it is not the most general way to solve the UG field equations. Even so, in [147] the authors

show that temperature fluctuations of the Cosmic Microwave Background (CMB) radiation, and specifically the Sachs–Wolfe effect [148] has a correction term given by a scalar metric perturbation that is demanded to be non–vanishing in UG. Assuming adiabatic fluctuations, the authors of the mentioned work found that the main difference between the GR and UG prediction is only a dipole–like term which is suppressed at large scale, and thus, the effect induced by UG is negligible. Moreover, in terms of gauge–invariant quantities, it was shown in [149] that the GR and UG cosmological perturbations are identical, and then, CMB photons will not distinguish between the two theories. An analysis including the non–conservation of the energy–momentum tensor has to be made in order to explore possible deviations of GR in cosmological observables such as CMB anisotropies and large scale structures.

While the discrepancies between early and late Universe in the H_0 measurements may be due to still unaccounted systematic errors in the observations, there exists the possibility that new physics is needed in order to unravel this cosmological conundrum. A deeper comprehension of the physical mechanisms driving the diffusion processes is needed in order to have a complete description of the non–gravitational interaction between the dark sector components. Nonetheless, the phenomenological models studied here might constitute a compelling variation to the Λ CDM paradigm. In this sense, Unimodular Gravity offers not only a explanation to the origin of the cosmological constant, but also the non–conservation of the energy–momentum tensor that naturally arises in this gravitational framework allows to address the H_0 tension successfully.

Acknowledgements

Francisco X. Linares Cedeño acknowledges the receipt of the grant from the Abdus Salam International Centre for Theoretical Physics, Trieste, Italy. FXLC also acknowledges CONACYT–SNI and the Programa para el Desarrollo Profesional Docente for financial support.

A Incomplete Gamma Function and the CSL model

The Continuous Spontaneous Localization (CSL) model leads to an expression for the CDM energy density that involves the following integral

$$I(t) \equiv \int_0^t e^{\xi_{CSL} t'} [1 + z(t')]^3 dt'. \quad (37)$$

We need to solve the background evolution to be able to give the explicit function $z(t)$, and thus, the Friedmann equation (21d) is an integro–differential equation,

$$\frac{1}{H_0^2 [1 + z(t)]^2} \left[\frac{dz(t)}{dt} \right]^2 = \Omega_r[z(t)] + \Omega_b[z(t)] + \Omega_{cdm}[z(t)] e^{\xi_{CSL} t} - \Omega_{cdm} \xi_{CSL} \int_0^t e^{\xi_{CSL} t'} [1 + z(t')]^3 dt' + \Omega_{\Lambda_{eff}}. \quad (38)$$

This will be the case even if we try to integrate $I(t)$ by parts: let be $f(t) \equiv [1 + z(t)]^3$, then

$$\begin{aligned} I(t) &= \left. \frac{f(t') e^{\xi_{CSL} t'}}{\xi_{CSL}} \right|_0^t - \int_0^t \frac{e^{\xi_{CSL} t'}}{\xi_{CSL}} \dot{f}(t') dt' \\ &= \frac{[1 + z(t)]^3 e^{\xi_{CSL} t}}{\xi_{CSL}} - \frac{1}{\xi_{CSL}} + \frac{3}{\xi_{CSL}} \int_0^t e^{\xi_{CSL} t'} [1 + z(t')]^3 H(t') dt'. \end{aligned} \quad (39)$$

A way to handle this situation, is by proposing an ansatz on the temporal dependence of the scale factor $a(t)$, or equivalently, the redshift $z(t)$. This is in fact usually done in the framework of Λ CDM model, where it is well–known that a power law relates the scale factor with the cosmic time as $a(t) = (t/t_0)^p$, with $p = 1/2$ ($p = 2/3$) for radiation (matter) domination era. Thus, considering that the new term arising from the CSL diffusion process will not change drastically such power law relation, let us propose

$$a(t) = \frac{1}{1 + z(t)} \equiv \left(\frac{t}{t_0} \right)^p, \quad (40)$$

and then the integral (37) is then written as

$$I(t) \equiv \int_0^t e^{\xi_{CSL} t'} \left(\frac{t'}{t_0} \right)^{-3p} dt'. \quad (41)$$

If we now introduce the following change of variable $u \equiv -\xi_{CSL}t$, we have

$$I_s(u) \equiv \frac{t_0}{u_0^s} \int_0^u e^{-u'} u'^{s-1} du', \quad (42)$$

where we have defined $-3p \equiv s - 1$, and $u_0 \equiv -\xi_{CSL}t_0$. The integral in the last expression looks like the *lower incomplete Gamma function* $\gamma(s, u)$ [150, 151, 152, 153], which has the following series representation [154, 155, 156]

$$\gamma(s, u) = \int_0^u e^{-u'} u'^{s-1} du' = \sum_{k=0}^{\infty} \frac{(-1)^k u^{k+s}}{k!(k+s)}, \quad \text{for } s > 0 \text{ and } u \geq 0. \quad (43)$$

Thus, it is mandatory to verify whether $\{u, s\}$ satisfy such conditions. Given the change of variable $u \equiv -\xi_{CSL}t$, we observe that $\xi_{CSL} \leq 0$ is needed to have $u \geq 0$. On the other hand, $s > 0$ implies $1 - 3p > 0$. Considering values of the diffusion constant such that $|\xi_{CSL}| \ll 1$, we expect that the power law given by the ansatz (40) does not differ too much from the Λ CDM result, and then $s = -1/2$ ($s = -1$) for radiation (matter) domination era. Moreover, it can be seen that the constant term out of the integral (42) will be imaginary in radiation domination if $\xi_{CSL} > 0$. This indicates that even when u will be well-defined for $\xi_{CSL} < 0$, the value of s in the cosmological context we are studying lies within the set of negative integers and negative semi-integers. Therefore, we can not identify our integral $I_s(u)$ in terms of $\gamma(s, u)$, at least in its standard form.

Before going further, let us summarize the above discussion as follows: the only case that will lead to an integral with physical meaning ($I_s(u) \in \mathbb{R}$), is when $\xi_{CSL} \leq 0 \Rightarrow u \geq 0$, with $s < 0$. Since the lower incomplete Gamma function $\gamma(s, u)$ does not admits negative values of the so-called *shape parameter* s , some sort of extension or generalization has to be implemented. This have been possible by using the tools of *Neutrix Calculus* [157, 158, 159], when studying the asymptotic behavior of divergent integrals. The main use of neutrix calculus and neutrix limit, is to extract the finite part of divergent quantities. This have been used, for example, in Quantum Field Theory to obtain finite renormalizations in loop calculations [160, 161]. Within this context, different generalizations to the standard and well-known lower incomplete Gamma function have been developed [162, 163, 164, 165, 166, 167, 168, 169]. Particularly in [163, 165, 168] have developed an extension to consider negative integers given by

$$\gamma(-s, u) = \frac{(-1)^s}{s!} \ln u + \sum_{\substack{k=0 \\ k \neq s}}^{\infty} \frac{(-1)^k u^{k-s}}{k!(k-s)}, \quad \text{for } s \in \mathbb{N} \text{ and } u > 0. \quad (44)$$

Since $s \in \mathbb{N}$, the above equation will be useful for the matter domination era, where we are interested in $\gamma(-1, u)$.

On the other hand, another way to write the lower incomplete Gamma function is given by its suitably normalized form [170, 171]

$$\gamma^*(s, u) = \frac{u^{-s}}{\Gamma(s)} \gamma(s, u). \quad (45)$$

Written like this, $\gamma^*(s, u)$ is a real-valued function for $s, u \in \mathbb{R}$ and such that $s, u > 0$. An extension of this formula was given in [172, 173] to consider negative and real values of s with $u > 0$, where particularly for $s \geq -1/2$ we have

$$\gamma^*(s, u) = \frac{1}{\Gamma(s+1)} \sum_{k=0}^{\infty} \frac{s(-u)^k}{k!(k+s)}. \quad (46)$$

Therefore, using Eq. (45) we have that

$$\gamma(s, u) = \frac{\Gamma(s)u^s}{\Gamma(s+1)} \sum_{k=0}^{\infty} \frac{s(-u)^k}{k!(k+s)}, \quad \text{for } s \geq -1/2 \text{ and } u > 0. \quad (47)$$

The last equation can then be used during the radiation domination era, where $s = -1/2$. Thus, the integral in Eq. (42) can be now formally identified with the *Generalized lower incomplete Gamma function* $\gamma^G(s, u)$ as follows,

$$I_s(u) = \frac{t_0}{u_0^s} \gamma^G(s, u), \quad \text{for } u > 0, \quad (48)$$

where, using the results of Eq. (44) and Eq. (47), we have

$$\gamma^G(s, u) = \begin{cases} \gamma(-1, u) = -\ln u + \sum_{\substack{k=0 \\ k \neq 1}}^{\infty} \frac{(-1)^k u^{k-1}}{k!(k-1)}, & \text{for } s = -1, \\ \gamma(-1/2, u) = -\frac{1}{u^{1/2}} \sum_{k=0}^{\infty} \frac{(-u)^k}{k!(k-1/2)}, & \text{for } s = -1/2, \end{cases} \quad (49)$$

where we have used that $\Gamma(1/2) = \sqrt{\pi}$ and $\Gamma(-1/2) = -2\sqrt{\pi}$. The Gamma function $\Gamma(s)$ is classically defined for positive integers, but it can be extended to both, real and imaginary numbers as well (see for instance [174]). Now, let us work on the series shown in Eq. (49).

A.1 $s = -1$

For matter domination era we have

$$\gamma^G(-1, u) = -\ln u + \sum_{\substack{k=0 \\ k \neq 1}}^{\infty} \frac{(-1)^k u^{k-1}}{k!(k-1)} \simeq -\ln u - \frac{1}{u} + \frac{u}{2} - \frac{u^2}{12} + \dots, \quad (50)$$

which as function of the redshift is written as

$$\gamma^G(-1, z) \simeq -\ln \left[\frac{u_0}{(1+z)^{3/2}} \right] - \frac{(1+z)^{3/2}}{u_0} + \frac{u_0}{2(1+z)^{3/2}} - \frac{u_0^2}{12(1+z)^3} + \dots \quad (51)$$

Then, Eq. (48) is given by

$$I_{-1}(z) \simeq -t_0 u_0 \ln \left[\frac{u_0}{(1+z)^{3/2}} \right] - t_0 (1+z)^{3/2} + \frac{t_0 u_0^2}{2(1+z)^{3/2}} - \frac{t_0 u_0^3}{12(1+z)^3} + \dots \quad (52)$$

Recalling that this integral has a multiplicative factor of ξ_{CSL} (see Eq. (38)), and considering the dimensionless variable $u_0 \equiv -\xi_{CSL} t_0$ as the parameter with which the expansion is developed,

$$\xi_{CSL} I_{-1}(z) \simeq u_0 (1+z)^{3/2} + u_0^2 \ln \left[\frac{u_0}{(1+z)^{3/2}} \right] - \frac{u_0^3}{2(1+z)^{3/2}} + \frac{u_0^4}{12(1+z)^3} + \dots, \quad \text{for } u_0 \ll 1. \quad (53)$$

Therefore, if we neglect terms of order equal and higher than $\mathcal{O}(u_0^2)$, we have that in the matter domination era, the modified Friedmann equation is written as

$$E(z) = \sqrt{\Omega_r(z) + \Omega_b(z) + \Omega_{cdm}(z) [e^{-u_0(1+z)^{-3/2}} - u_0(1+z)^{-3/2}] + \Omega_{\Lambda_{eff}}}. \quad (54)$$

A.2 $s = -1/2$

In the case of the radiation domination era, Eq. (49) reads as follows,

$$\gamma^G(-1/2, u) = -\frac{1}{u^{1/2}} \sum_{k=0}^{\infty} \frac{(-u)^k}{k!(k-1/2)} \simeq \frac{2}{u^{1/2}} + 2u^{1/2} - \frac{u^{3/2}}{3} + \frac{u^{5/2}}{15} + \dots \quad (55)$$

When the above expression is written in terms of the redshift we have

$$\gamma^G(-1/2, z) \simeq \frac{2(1+z)}{u_0^{1/2}} + \frac{2u_0^{1/2}}{1+z} - \frac{u_0^{3/2}}{3(1+z)^3} + \frac{u_0^{5/2}}{15(1+z)^5} + \dots, \quad (56)$$

which leads to the integral (48)

$$\xi_{CSL} I_{-1/2}(z) \simeq -2u_0(1+z) - \frac{2u_0^2}{1+z} + \frac{u_0^3}{3(1+z)^3} - \frac{u_0^4}{15(1+z)^5} + \dots \quad (57)$$

where we have already included the multiplicative factor ξ_{CSL} . Again, neglecting terms of order $\mathcal{O}(u_0^2)$ and higher, the Friedmann equation is written as

$$E(z) = \sqrt{\Omega_r(z) + \Omega_b(z) + \Omega_{cdm}(z) [e^{-u_0(1+z)^{-2}} + 2u_0(1+z)^{-2}] + \Omega_{\Lambda_{eff}}}. \quad (58)$$

Therefore, the Friedmann equation for the CSL model, can be written as Eq. (54) and (58) for matter domination and radiation domination respectively, as is shown in Eq. (21e).

References

- [1] Clifford M. Will. The Confrontation between General Relativity and Experiment. *Living Rev. Rel.*, 17:4, 2014.
- [2] Clifford M. Will. Putting General Relativity to the Test: Twentieth-Century Highlights and Twenty-First-Century Prospects. *Einstein Stud.*, 14:81–96, 2018.
- [3] Adam G. Riess, i in. Observational evidence from supernovae for an accelerating universe and a cosmological constant. *Astron. J.*, 116:1009–1038, 1998.
- [4] S. Perlmutter, i in. Measurements of Omega and Lambda from 42 high redshift supernovae. *Astrophys. J.*, 517:565–586, 1999.
- [5] Daniel J. Eisenstein, i in. Detection of the Baryon Acoustic Peak in the Large-Scale Correlation Function of SDSS Luminous Red Galaxies. *Astrophys. J.*, 633:560–574, 2005.
- [6] David Parkinson, i in. The WiggleZ Dark Energy Survey: Final data release and cosmological results. *Phys. Rev.*, D86:103518, 2012.
- [7] N. Aghanim, i in. Planck 2018 results. VI. Cosmological parameters. *Astron. Astrophys.*, 641:A6, 2020.
- [8] Daniela Carturan, Fabio Finelli. Cosmological effects of a class of fluid dark energy models. *Phys. Rev. D*, 68:103501, 2003.
- [9] Vincenzo F. Cardone, C. Tortora, A. Troisi, S. Capozziello. Beyond the perfect fluid hypothesis for dark energy equation of state. *Phys. Rev. D*, 73:043508, 2006.
- [10] Shin’ichi Nojiri, Sergei D. Odintsov. The New form of the equation of state for dark energy fluid and accelerating universe. *Phys. Lett. B*, 639:144–150, 2006.
- [11] Iver H. Brevik, O.G. Gorbunova, A.V. Timoshkin. Dark energy fluid with time-dependent, inhomogeneous equation of state. *Eur. Phys. J. C*, 51:179–183, 2007.
- [12] Eric V. Linder, Robert J. Scherrer. Aetherizing Lambda: Barotropic Fluids as Dark Energy. *Phys. Rev. D*, 80:023008, 2009.
- [13] Xiaoxian Duan, Yichao Li, Changjun Gao. Constraining the Lattice Fluid Dark Energy from SNe Ia, BAO and OHD. *Sci. China Phys. Mech. Astron.*, 56:1220–1226, 2013.
- [14] Donato Bini, Andrea Geralico, Daniele Gregoris, Sauro Succi. Dark energy from cosmological fluids obeying a Shan-Chen nonideal equation of state. *Phys. Rev. D*, 88(6):063007, 2013.
- [15] Cristian Barrera-Hinojosa, Domenico Sapone. Relativistic effects in the large-scale structure with effective dark energy fluids. *JCAP*, 03:037, 2020.
- [16] R. R. Caldwell. A Phantom menace? *Phys. Lett.*, B545:23–29, 2002.
- [17] Robert R. Caldwell, Marc Kamionkowski, Nevin N. Weinberg. Phantom energy and cosmic doomsday. *Phys. Rev. Lett.*, 91:071301, 2003.
- [18] Shin’ichi Nojiri, Sergei D. Odintsov, Shinji Tsujikawa. Properties of singularities in (phantom) dark energy universe. *Phys. Rev.*, D71:063004, 2005.
- [19] Bo Feng. The quintom model of dark energy. *Proceedings, fifteenth Workshop on General Relativity and Gravitation in Japan, JGRG 15, Tokyo Institute of Technology, Tokyo, Japan, November 28 - December 2, 2005*, 2006.
- [20] Eric V. Linder. The Dynamics of Quintessence, The Quintessence of Dynamics. *Gen. Rel. Grav.*, 40:329–356, 2008.
- [21] M. R. Setare, E. N. Saridakis. Quintom dark energy models with nearly flat potentials. *Phys. Rev.*, D79:043005, 2009.
- [22] Shinji Tsujikawa. Quintessence: A Review. *Class. Quant. Grav.*, 30:214003, 2013.
- [23] Takeshi Chiba, Antonio De Felice, Shinji Tsujikawa. Observational constraints on quintessence: thawing, tracker, and scaling models. *Phys. Rev.*, D87(8):083505, 2013.
- [24] Andrei Linde. Single-field α -attractors. *JCAP*, 1505:003, 2015.
- [25] Eric V. Linder. Dark Energy from α -Attractors. *Phys. Rev.*, D91(12):123012, 2015.
- [26] Jean-Baptiste Durrive, Junpei Ooba, Kiyotomo Ichiki, Naoshi Sugiyama. Updated observational constraints on quintessence dark energy models. *Phys. Rev.*, D97(4):043503, 2018.
- [27] Satadru Bag, Swagat S. Mishra, Varun Sahni. New tracker models of dark energy. *JCAP*, 08:009, 2018.

- [28] Genly Leon, Andronikos Paliathanasis, Jorge Luis Morales-Martínez. The past and future dynamics of quintom dark energy models. *Eur. Phys. J.*, C78(9):753, 2018.
- [29] Carlos García-García, Eric V. Linder, Pilar Ruíz-Lapuente, Miguel Zumalacárregui. Dark energy from α -attractors: phenomenology and observational constraints. *JCAP*, 08:022, 2018.
- [30] Timothy Clifton, Pedro G. Ferreira, Antonio Padilla, Constantinos Skordis. Modified Gravity and Cosmology. *Phys. Rept.*, 513:1–189, 2012.
- [31] Ivan Dimitrijevic, Branko Dragovich, Jelena Grujic, Zoran Rakic. On Modified Gravity. *Springer Proc. Math. Stat.*, 36:251–259, 2013.
- [32] Philippe Brax, Anne-Christine Davis. Distinguishing modified gravity models. *JCAP*, 1510(10):042, 2015.
- [33] Austin Joyce, Lucas Lombriser, Fabian Schmidt. Dark Energy Versus Modified Gravity. *Ann. Rev. Nucl. Part. Sci.*, 66:95–122, 2016.
- [34] Luisa G. Jaime, Mariana Jaber, Celia Escamilla-Rivera. New parametrized equation of state for dark energy surveys. *Phys. Rev.*, D98(8):083530, 2018.
- [35] Anže Slosar, i in. Dark Energy and Modified Gravity. 2019.
- [36] Albert Einstein. Cosmological Considerations in the General Theory of Relativity. *Sitzungsber. Preuss. Akad. Wiss. Berlin (Math. Phys.)*, 1917:142–152, 1917.
- [37] Edwin Hubble. A relation between distance and radial velocity among extra-galactic nebulae. *Proc. Nat. Acad. Sci.*, 15:168–173, 1929.
- [38] Albert Einstein. The Formal Foundation of the General Theory of Relativity. *Sitzungsber. Preuss. Akad. Wiss. Berlin (Math. Phys.)*, 1914:1030–1085, 1914.
- [39] Albert Einstein. Spielen Gravitationsfelder im Aufbau der materiellen Elementarteilchen eine wesentliche Rolle? *Sitzungsber. Preuss. Akad. Wiss. Berlin (Math. Phys.)*, 1919:349–356, 1919.
- [40] J. L. Anderson, D. Finkelstein. Cosmological constant and fundamental length. *Am. J. Phys.*, 39:901–904, 1971.
- [41] J. J. van der Bij, H. van Dam, Yee Jack Ng. The Exchange of Massless Spin Two Particles. *Physica*, 116A:307–320, 1982.
- [42] Steven Weinberg. The Cosmological Constant Problem. *Rev. Mod. Phys.*, 61:1–23, 1989. [,569(1988)].
- [43] W. Buchmuller, N. Dragon. Einstein Gravity From Restricted Coordinate Invariance. *Phys. Lett.*, B207:292–294, 1988.
- [44] W. Buchmuller, N. Dragon. Gauge Fixing and the Cosmological Constant. *Phys. Lett.*, B223:313–317, 1989.
- [45] Y. Jack Ng, H. van Dam. Unimodular Theory of Gravity and the Cosmological Constant. *J. Math. Phys.*, 32:1337–1340, 1991.
- [46] Lee Smolin. The Quantization of unimodular gravity and the cosmological constant problems. *Phys. Rev. D*, 80:084003, 2009.
- [47] Astrid Eichhorn. On unimodular quantum gravity. *Class. Quant. Grav.*, 30:115016, 2013.
- [48] E. Álvarez, S. González-Martín, M. Herrero-Valea, C.P. Martín. Unimodular Gravity Redux. *Phys. Rev. D*, 92(6):061502, 2015.
- [49] R. Bufalo, M. Oksanen, A. Tureanu. How unimodular gravity theories differ from general relativity at quantum level. *Eur. Phys. J. C*, 75(10):477, 2015.
- [50] R. Percacci. Unimodular quantum gravity and the cosmological constant. *Found. Phys.*, 48(10):1364–1379, 2018.
- [51] Pankaj Jain, Atul Jaiswal, Purnendu Karmakar, Gopal Kashyap, Naveen K. Singh. Cosmological implications of unimodular gravity. *JCAP*, 11:003, 2012.
- [52] George F R Ellis. The Trace-Free Einstein Equations and inflation. *Gen. Rel. Grav.*, 46:1619, 2014.
- [53] A.O. Barvinsky, A. Yu. Kamenshchik. Darkness without dark matter and energy – generalized unimodular gravity. *Phys. Lett. B*, 774:59–63, 2017.
- [54] Miguel A. García-Aspeitia, C. Martínez-Robles, A. Hernández-Almada, Juan Magaña, V. Motta. Cosmic acceleration in unimodular gravity. *Phys. Rev. D*, 99(12):123525, 2019.
- [55] Miguel A. García-Aspeitia, A. Hernández-Almada, Juan Magaña, V. Motta. On the birth of the cosmological constant and the reionization era. 12 2019.

- [56] A.O. Barvinsky, N. Kolganov. Inflation in generalized unimodular gravity. *Phys. Rev. D*, 100(12):123510, 2019.
- [57] A.O. Barvinsky, N. Kolganov, A. Kurov, D. Nesterov. Dynamics of the generalized unimodular gravity theory. *Phys. Rev. D*, 100(2):023542, 2019.
- [58] Alejandro Perez, Daniel Sudarsky, Edward Wilson-Ewing. Resolving the H_0 tension with diffusion. 2020.
- [59] Cristóbal Corral, Norman Cruz, Esteban González. Diffusion in unimodular gravity: Analytical solutions, late-time acceleration, and cosmological constraints. *Phys. Rev. D*, 102(2):023508, 2020.
- [60] George F. R. Ellis, Henk van Elst, Jeff Murugan, Jean-Philippe Uzan. On the Trace-Free Einstein Equations as a Viable Alternative to General Relativity. *Class. Quant. Grav.*, 28:225007, 2011.
- [61] Thibaut Josset, Alejandro Perez, Daniel Sudarsky. Dark Energy from Violation of Energy Conservation. *Phys. Rev. Lett.*, 118(2):021102, 2017.
- [62] Luca Amendola. Perturbations in a coupled scalar field cosmology. *Mon. Not. Roy. Astron. Soc.*, 312:521, 2000.
- [63] Luca Amendola. Coupled quintessence. *Phys. Rev. D*, 62:043511, 2000.
- [64] Andrew P. Billyard, Alan A. Coley. Interactions in scalar field cosmology. *Phys. Rev. D*, 61:083503, 2000.
- [65] German Olivares, Fernando Atrio-Barandela, Diego Pavon. Observational constraints on interacting quintessence models. *Phys. Rev. D*, 71:063523, 2005.
- [66] German Olivares, Fernando Atrio-Barandela, Diego Pavon. Dynamics of Interacting Quintessence Models: Observational Constraints. *Phys. Rev. D*, 77:063513, 2008.
- [67] Gabriela Caldera-Cabral, Roy Maartens, L. Arturo Urena-Lopez. Dynamics of interacting dark energy. *Phys. Rev. D*, 79:063518, 2009.
- [68] Laura Lopez Honorez, Olga Mena, Grigoris Panotopoulos. Higher-order coupled quintessence. *Phys. Rev. D*, 82:123525, 2010.
- [69] Supriya Pan, Subhra Bhattacharya, Subenoy Chakraborty. An analytic model for interacting dark energy and its observational constraints. *Mon. Not. Roy. Astron. Soc.*, 452(3):3038–3046, 2015.
- [70] Valentina Salvatelli, Andrea Marchini, Laura Lopez-Honorez, Olga Mena. New constraints on Coupled Dark Energy from the Planck satellite experiment. *Phys. Rev. D*, 88(2):023531, 2013.
- [71] Yu. L. Bolotin, A. Kostenko, O.A. Lemets, D.A. Yerokhin. Cosmological Evolution With Interaction Between Dark Energy And Dark Matter. *Int. J. Mod. Phys. D*, 24(03):1530007, 2014.
- [72] Supriya Pan, G.S. Sharov. A model with interaction of dark components and recent observational data. *Mon. Not. Roy. Astron. Soc.*, 472(4):4736–4749, 2017.
- [73] Mariana Carrillo González, Mark Trodden. Field Theories and Fluids for an Interacting Dark Sector. *Phys. Rev. D*, 97(4):043508, 2018. [Erratum: *Phys. Rev. D* 101, 089901 (2020)].
- [74] Bruno J. Barros, Luca Amendola, Tiago Barreiro, Nelson J. Nunes. Coupled quintessence with a Λ CDM background: removing the σ_8 tension. *JCAP*, 01:007, 2019.
- [75] Weiqiang Yang, Olga Mena, Supriya Pan, Eleonora Di Valentino. Dark sectors with dynamical coupling. *Phys. Rev. D*, 100(8):083509, 2019.
- [76] Weiqiang Yang, Eleonora Di Valentino, Olga Mena, Supriya Pan. Dynamical Dark sectors and Neutrino masses and abundances. *Phys. Rev. D*, 102(2):023535, 2020.
- [77] Mahnaz Asghari, Shahram Khosravi, Amir Mollazadeh. Perturbation level interacting dark energy model and its consequence on late-time cosmological parameters. *Phys. Rev. D*, 101(4):043503, 2020.
- [78] Joseph P. Johnson, S. Shankaranarayanan. Cosmological perturbations in the interacting dark sector: Mapping fields and fluids. 6 2020.
- [79] Eleonora Di Valentino, Alessandro Melchiorri, Olga Mena. Can interacting dark energy solve the H_0 tension? *Phys. Rev. D*, 96(4):043503, 2017.
- [80] Weiqiang Yang, Ankan Mukherjee, Eleonora Di Valentino, Supriya Pan. Interacting dark energy with time varying equation of state and the H_0 tension. *Phys. Rev. D*, 98(12):123527, 2018.
- [81] Weiqiang Yang, Supriya Pan, Eleonora Di Valentino, Rafael C. Nunes, Sunny Vagnozzi, David F. Mota. Tale of stable interacting dark energy, observational signatures, and the H_0 tension. *JCAP*, 09:019, 2018.
- [82] Eleonora Di Valentino, Alessandro Melchiorri, Olga Mena, Sunny Vagnozzi. Interacting dark energy in the early 2020s: A promising solution to the H_0 and cosmic shear tensions. *Phys. Dark Univ.*, 30:100666, 2020.

- [83] Supriya Pan, Weiqiang Yang, Eleonora Di Valentino, Emmanuel N. Saridakis, Subenoy Chakraborty. Interacting scenarios with dynamical dark energy: Observational constraints and alleviation of the H_0 tension. *Phys. Rev. D*, 100(10):103520, 2019.
- [84] Adrià Gómez-Valent, Valeria Pettorino, Luca Amendola. Update on coupled dark energy and the H_0 tension. *Phys. Rev. D*, 101(12):123513, 2020.
- [85] Matteo Lucca, Deanna C. Hooper. Tensions in the dark: shedding light on Dark Matter-Dark Energy interactions. 2 2020.
- [86] Supriya Pan, Weiqiang Yang, Andronikos Paliathanasis. Non-linear interacting cosmological models after Planck 2018 legacy release and the H_0 tension. *Mon. Not. Roy. Astron. Soc.*, 493(3):3114–3131, 2020.
- [87] Wendy L. Freedman. Cosmology at at Crossroads: Tension with the Hubble Constant. *Nat. Astron.*, 1:0169, 2017.
- [88] L. Verde, T. Treu, A. G. Riess. Tensions between the Early and the Late Universe. *Nature Astronomy* 2019, 2019.
- [89] Simone Aiola, i in. The Atacama Cosmology Telescope: DR4 Maps and Cosmological Parameters. 7 2020.
- [90] T.M.C. Abbott, i in. Dark Energy Survey Year 1 Results: A Precise H_0 Estimate from DES Y1, BAO, and D/H Data. *Mon. Not. Roy. Astron. Soc.*, 480(3):3879–3888, 2018.
- [91] Oliver H.E. Philcox, Mikhail M. Ivanov, Marko Simonović, Matias Zaldarriaga. Combining Full-Shape and BAO Analyses of Galaxy Power Spectra: A 1.6% CMB-independent constraint on H_0 . *JCAP*, 05:032, 2020.
- [92] Adam G. Riess, Stefano Casertano, Wenlong Yuan, Lucas M. Macri, Dan Scolnic. Large Magellanic Cloud Cepheid Standards Provide a 1% Foundation for the Determination of the Hubble Constant and Stronger Evidence for Physics beyond Λ CDM. *Astrophys. J.*, 876(1):85, 2019.
- [93] Wendy L. Freedman, i in. The Carnegie-Chicago Hubble Program. VIII. An Independent Determination of the Hubble Constant Based on the Tip of the Red Giant Branch. 7 2019.
- [94] Wendy L. Freedman, Barry F. Madore, Taylor Hoyt, In Sung Jang, Rachael Beaton, Myung Gyoong Lee, Andrew Monson, Jill Neeley, Jeffrey Rich. Calibration of the Tip of the Red Giant Branch (TRGB). 2 2020.
- [95] Caroline D. Huang, Adam G. Riess, Wenlong Yuan, Lucas M. Macri, Nadia L. Zakamska, Stefano Casertano, Patricia A. Whitelock, Samantha L. Hoffmann, Alexei V. Filippenko, Daniel Scolnic. Hubble Space Telescope Observations of Mira Variables in the Type Ia Supernova Host NGC 1559: An Alternative Candle to Measure the Hubble Constant. 8 2019.
- [96] Kenneth C. Wong, i in. H0LiCOW XIII. A 2.4% measurement of H_0 from lensed quasars: 5.3σ tension between early and late-Universe probes. 7 2019.
- [97] D.W. Pesce, i in. The Megamaser Cosmology Project. XIII. Combined Hubble constant constraints. *Astrophys. J. Lett.*, 891(1):L1, 2020.
- [98] Cicely Potter, Joseph B Jensen, John Blakeslee, Peter Milne, Peter M Garnavich, Peter Brown. Calibrating the type ia supernova distance scale using surface brightness fluctuations. *American Astronomical Society Meeting Abstracts# 232*, wolumen 232, 2018.
- [99] Vivien Bonvin, Martin Millon. H0licow h_0 tension plotting notebook, Luty 2020.
- [100] Simone Calogero, Hermano Velten. Cosmology with matter diffusion. *JCAP*, 1311:025, 2013.
- [101] Zbigniew Haba, Aleksander Stachowski, Marek Szydlowski. Dynamics of the diffusive DM-DE interaction – Dynamical system approach. *JCAP*, 07:024, 2016.
- [102] David Benisty, E.I. Guendelman. Unified DE–DM with diffusive interactions scenario from scalar fields. *Int. J. Mod. Phys. D*, 26(12):1743021, 2017.
- [103] David Benisty, E. I. Guendelman. Interacting Diffusive Unified Dark Energy and Dark Matter from Scalar Fields. *Eur. Phys. J.*, C77(6):396, 2017.
- [104] David Benisty, Eduardo Guendelman, Zbigniew Haba. Unification of dark energy and dark matter from diffusive cosmology. *Phys. Rev.*, D99(12):123521, 2019. [Erratum: *Phys. Rev.*D101,no.4,049901(2020)].
- [105] Julien Lesgourgues. The Cosmic Linear Anisotropy Solving System (CLASS) I: Overview. 2011.
- [106] Philip M. Pearle. Reduction of the State Vector by a Nonlinear Schrodinger Equation. *Phys. Rev. D*, 13:857–868, 1976.
- [107] Philip M. Pearle. Combining Stochastic Dynamical State Vector Reduction With Spontaneous Localization. *Phys. Rev. A*, 39:2277–2289, 1989.

- [108] Gian Carlo Ghirardi, Philip M. Pearle, Alberto Rimini. Markov Processes in Hilbert Space and Continuous Spontaneous Localization of Systems of Identical Particles. *Phys. Rev. A*, 42:78–79, 1990.
- [109] Angelo Bassi, Gian Carlo Ghirardi. Dynamical reduction models. *Phys. Rept.*, 379:257, 2003.
- [110] Alejandro Perez, Hanno Sahlmann, Daniel Sudarsky. On the quantum origin of the seeds of cosmic structure. *Class. Quant. Grav.*, 23:2317–2354, 2006.
- [111] Kinjalk Lochan, Suratna Das, Angelo Bassi. Constraining CSL strength parameter λ from standard cosmology and spectral distortions of CMBR. *Phys. Rev. D*, 86:065016, 2012.
- [112] Jerome Martin, Vincent Vennin, Patrick Peter. Cosmological Inflation and the Quantum Measurement Problem. *Phys. Rev. D*, 86:103524, 2012.
- [113] Pedro Cañate, Philip Pearle, Daniel Sudarsky. Continuous spontaneous localization wave function collapse model as a mechanism for the emergence of cosmological asymmetries in inflation. *Phys. Rev. D*, 87(10):104024, 2013.
- [114] María Pía Piccirilli, Gabriel León, Susana J. Landau, Micol Benetti, Daniel Sudarsky. Constraining quantum collapse inflationary models with current data: The semiclassical approach. *Int. J. Mod. Phys. D*, 28(02):1950041, 2018.
- [115] Gabriel León, Abhishek Majhi, Elias Okon, Daniel Sudarsky. Expectation of primordial gravity waves generated during inflation. *Phys. Rev. D*, 98(2):023512, 2018.
- [116] Gabriel Leon, Maria Pia Piccirilli. Generation of inflationary perturbations in the continuous spontaneous localization model: The second order power spectrum. *Phys. Rev. D*, 102(4):043515, 2020.
- [117] Stephen L Adler, Angelo Bassi. Collapse models with non-white noises. *Journal of Physics A: Mathematical and Theoretical*, 40(50):15083–15098, nov 2007.
- [118] Stephen L Adler, Angelo Bassi. Collapse models with non-white noises: II. particle-density coupled noises. *Journal of Physics A: Mathematical and Theoretical*, 41(39):395308, sep 2008.
- [119] Juan Magana, Mario H. Amante, Miguel A. Garcia-Aspeitia, V. Motta. The Cardassian expansion revisited: constraints from updated Hubble parameter measurements and type Ia supernova data. *Mon. Not. Roy. Astron. Soc.*, 476(1):1036–1049, 2018.
- [120] D.M. Scolnic, i in. The Complete Light-curve Sample of Spectroscopically Confirmed SNe Ia from Pan-STARRS1 and Cosmological Constraints from the Combined Pantheon Sample. *Astrophys. J.*, 859(2):101, 2018.
- [121] Lu Chen, Qing-Guo Huang, Ke Wang. Distance Priors from Planck Final Release. *JCAP*, 1902:028, 2019.
- [122] Mohammad Malekjani, Mehdi Rezaei, Iman A. Akhlaghi. Can Holographic dark energy models fit the observational data? *Phys. Rev.*, D98(6):063533, 2018.
- [123] Francisco X. Linares Cedeño, Ariadna Montiel, Juan Carlos Hidalgo, Gabriel Germán. Bayesian evidence for α -attractor dark energy models. *JCAP*, 1908(08):002, 2019.
- [124] Alexander Bonilla Rivera, Jorge Enrique García-Farieta. Exploring the Dark Universe: constraints on dynamical Dark Energy models from CMB, BAO and growth rate measurements. *Int. J. Mod. Phys.*, D28(09):1950118, 2019.
- [125] Xiaolei Li, Arman Shafieloo, Varun Sahni, Alexei A. Starobinsky. Revisiting Metastable Dark Energy and Tensions in the Estimation of Cosmological Parameters. *Astrophys. J.*, 887:153, 2019.
- [126] Xiaolei Li, Arman Shafieloo. A Simple Phenomenological Emergent Dark Energy Model can Resolve the Hubble Tension. *Astrophys. J.*, 883(1):L3, 2019. [*Astrophys. J. Lett.*883,L3(2019)].
- [127] Zahra Davari, Valerio Marra, Mohammad Malekjani. Cosmological constraints on minimally and non-minimally coupled scalar field models. *Mon. Not. Roy. Astron. Soc.*, 491(2):1920–1933, 2020.
- [128] Ariadna Montiel, J. I. Cabrera, Juan Carlos Hidalgo. Improving sampling and calibration of GRBs as distance indicators. 2020.
- [129] Benjamin Audren, Julien Lesgourgues, Karim Benabed, Simon Prunet. Conservative Constraints on Early Cosmology: an illustration of the Monte Python cosmological parameter inference code. *JCAP*, 1302:001, 2013.
- [130] Andrew Gelman, Donald B. Rubin. Inference from Iterative Simulation Using Multiple Sequences. *Statist. Sci.*, 7:457–472, 1992.
- [131] Stefan Taubenberger, Sherry H. Suyu. H0licow distance likelihoods in montepython, Luty 2020.

- [132] S.H. Suyu, P.J. Marshall, M.W. Auger, S. Hilbert, R.D. Blandford, L.V.E. Koopmans, C.D. Fassnacht, T. Treu. Dissecting the Gravitational Lens B1608+656. II. Precision Measurements of the Hubble Constant, Spatial Curvature, and the Dark Energy Equation of State. *Astrophys. J.*, 711:201–221, 2010.
- [133] S.H. Suyu, i in. Cosmology from gravitational lens time delays and Planck data. *Astrophys. J.*, 788:L35, 2014.
- [134] Kenneth C. Wong, i in. H0LiCOW – IV. Lens mass model of HE 0435–1223 and blind measurement of its time-delay distance for cosmology. *Mon. Not. Roy. Astron. Soc.*, 465(4):4895–4913, 2017.
- [135] S. Birrer, i in. H0LiCOW - IX. Cosmographic analysis of the doubly imaged quasar SDSS 1206+4332 and a new measurement of the Hubble constant. *Mon. Not. Roy. Astron. Soc.*, 484:4726, 2019.
- [136] Inh Jee, Sherry Suyu, Eiichiro Komatsu, Christopher D. Fassnacht, Stefan Hilbert, Léon V.E. Koopmans. A measurement of the Hubble constant from angular diameter distances to two gravitational lenses. 9 2019.
- [137] Geoff C.-F. Chen, i in. A SHARP view of H0LiCOW: H_0 from three time-delay gravitational lens systems with adaptive optics imaging. *Mon. Not. Roy. Astron. Soc.*, 490(2):1743–1773, 2019.
- [138] Cristian E. Rusu, i in. H0LiCOW XII. Lens mass model of WFI2033-4723 and blind measurement of its time-delay distance and H_0 . 5 2019.
- [139] David Camarena, Valerio Marra. Impact of the cosmic variance on H_0 on cosmological analyses. *Phys. Rev. D*, 98(2):023537, 2018.
- [140] M. Betoule, i in. Improved cosmological constraints from a joint analysis of the SDSS-II and SNLS supernova samples. *Astron. Astrophys.*, 568:A22, 2014.
- [141] Richard Kessler, Dan Scolnic. Correcting Type Ia Supernova Distances for Selection Biases and Contamination in Photometrically Identified Samples. *Astrophys. J.*, 836(1):56, 2017.
- [142] D.O. Jones, i in. Should Type Ia Supernova Distances be Corrected for their Local Environments? *Astrophys. J.*, 867(2):108, 2018.
- [143] Sherry H. Suyu, Tzu-Ching Chang, Frédéric Courbin, Teppei Okumura. Cosmological distance indicators. *Space Sci. Rev.*, 214(5):91, 2018.
- [144] Jérôme Martin, Vincent Vennin. Cosmic Microwave Background Constraints Cast a Shadow On Continuous Spontaneous Localization Models. *Phys. Rev. Lett.*, 124(8):080402, 2020.
- [145] Fay Dowker, Joe Henson, Rafael D. Sorkin. Quantum gravity phenomenology, Lorentz invariance and discreteness. *Mod. Phys. Lett. A*, 19:1829–1840, 2004.
- [146] Lydia Philpott, Fay Dowker, Rafael D. Sorkin. Energy-momentum diffusion from spacetime discreteness. *Phys. Rev. D*, 79:124047, 2009.
- [147] Caixia Gao, Robert H. Brandenberger, Yifu Cai, Pisin Chen. Cosmological Perturbations in Unimodular Gravity. *JCAP*, 09:021, 2014.
- [148] R.K. Sachs, A.M. Wolfe. Perturbations of a cosmological model and angular variations of the microwave background. *Astrophys. J.*, 147:73–90, 1967.
- [149] Abhishek Basak, Ophélie Fabre, S. Shankaranarayanan. Cosmological perturbations of unimodular gravity and general relativity are identical. *Gen. Rel. Grav.*, 48(10):123, 2016.
- [150] Milton Abramowitz, Irene A Stegun. Handbook of mathematical functions dover publications. *New York*, strona 361, 1965.
- [151] Walter Gautschi. The incomplete gamma functions since tricoli. In *Tricoli's Ideas and Contemporary Applied Mathematics, Atti dei Convegni Lincei, n. 147, Accademia Nazionale dei Lincei*, strongy 203–237, 1998.
- [152] Frank WJ Olver, Daniel W Lozier, Ronald F Boisvert, Charles W Clark. *NIST handbook of mathematical functions hardback and CD-ROM*. Cambridge university press, 2010.
- [153] G. J. O. Jameson. The incomplete gamma functions. *The Mathematical Gazette*, 100(548):298–306, 2016.
- [154] Edwin Plimpton Adams, Richard Lionel Hippiusley. *Smithsonian mathematical formulae and tables of elliptic functions*, wolumen 2672. Smithsonian institution, 1922.
- [155] A. Erdelyi. *Higher Transcendental Functions*, strona 59. 1953.
- [156] Izrail Solomonovich Gradshteyn, Iosif Moiseevich Ryzhik. *Table of integrals, series, and products*. Academic press, 2014.
- [157] J Hadamard. Lectures on cauchy's problem in linear partial differential equations, yale univ. *Press. New Haven*, 1923.

- [158] JG Van der Corput. Introduction to the neutrix calculus. *Journal d'Analyse Mathématique*, 7(1):281–398, 1959.
- [159] B Fisher. Neutrices and the product of distributions. *Studia Mathematica*, 57:263–274, 1976.
- [160] Y.Jack Ng, H. van Dam. Neutrix calculus and finite quantum field theory. *J. Phys. A*, 38:L317, 2005.
- [161] Y.Jack Ng, H. van Dam. An Application of neutrix calculus to quantum field theory. *Int. J. Mod. Phys. A*, 21:297–312, 2006.
- [162] M.Aslam Chaudhry, S.M. Zubair. Generalized incomplete gamma functions with applications. *Journal of Computational and Applied Mathematics*, 55(1):99 – 123, 1994.
- [163] Brian Fisher, Biljana Jolevsaka-Tuneska, Adem KiliÇman. On defining the incomplete gamma function. *Integral Transforms and Special Functions*, 14(4):293–299, 2003.
- [164] Brian Fisher. On defining the incomplete gamma function $\gamma(-m, x)$. *Integral Transforms and Special Functions*, 15(6):467–476, 2004.
- [165] Emin Özçağ, İ Ege, Haşmet Gürçay, Biljana Jolevska-Tuneska. Some remarks on the incomplete gamma function. *Mathematical Methods in Engineering*, strony 97–108. Springer, 2007.
- [166] Brian Fisher, Adem Kılıcman. Some results on the gamma function for negative integers. *Appl. Math. Inform. Sci*, 6(2):173–176, 2012.
- [167] Ian Thompson. Algorithm 926: Incomplete gamma functions with negative arguments. *ACM Transactions on Mathematical Software (TOMS)*, 39(2):1–9, 2013.
- [168] Emin Özçağ, İnci Ege. Remarks on polygamma and incomplete gamma type functions. *Journal of Number Theory*, 169:369–387, 2016.
- [169] Mongkolseri Lin, Brian Fisher, Somsak Orankitjaroen. On the incomplete gamma function and its neutrix convolution for negative integers. *Eurasian Mathematical Journal*, 10(1):30–51, 2019.
- [170] Paul Eugen Böhmer. *Differenzengleichung und bestimmte Integrale*. KF Koehler, 1939.
- [171] FG Tricomi. Asymptotische eigenschaften der unvollständigen gammafunktion. *Mathematische Zeitschrift*, 53(2):136–148, 1950.
- [172] Walter Gautschi. An evaluation procedure for incomplete gamma functions. Raport instytutowy, WISCONSIN UNIV MADISON MATHEMATICS RESEARCH CENTER, 1977.
- [173] Walter Gautschi. A computational procedure for incomplete gamma functions. *ACM Transactions on Mathematical Software (TOMS)*, 5(4):466–481, 1979.
- [174] Ashwani K Thukral. Factorials of real negative and imaginary numbers-a new perspective. *SpringerPlus*, 3(1):658, 2014.